The link between antibodies to OxLDL and natural protection against pneumococci depends on D_H gene conservation

Andre M. Vale,[1,5] Pratibha Kapoor,[1] Greg A. Skibinski,[2] Ada Elgavish,[1] Tamer I. Mahmoud,[2,7] Cosima Zemlin,[1] Michael Zemlin,[2,6] Peter D. Burrows,[2,5] Alberto Nobrega,[5] John F. Kearney,[2] David E. Briles,[2,3] and Harry W. Schroeder Jr.[1,2,4]

[1]Department of Medicine, [2]Department of Microbiology, [3]Department of Pediatrics, and [4]Department of Genetics, University of Alabama at Birmingham, Birmingham, AL 35294
[5]Instituto de Microbiologia Paulo de Góes, Universidade Federal do Rio de Janeiro, Rio de Janeiro 21941-901, Brazil
[6]Department of Pediatrics, Philipps University Marburg, D-35032 Marburg, Germany
[7]Department of Microbiology and Immunology, Faculty of Pharmacy, Cairo University, Cairo 11562, Egypt

Selection and physiological production of protective natural antibodies (NAbs) have been associated with exposure to endogenous antigens. The extent to which this association depends on germline NAb sequence is uncertain. Here we show that alterations in germline D_H sequence can sever the association between the production of self-reactive NAbs and NAbs that afford protection against a pathogen. In unmanipulated hosts, the availability of the evolutionarily conserved *DFL16.1* gene segment sequence profoundly affected the serum levels of NAbs against bacterial phosphorylcholine but not oxidized low-density lipoprotein. Mice with partially altered *DFL16.1* sequence could use N nucleotides to recreate the amino acid sequence associated with the classical protective T15 idiotype–positive NAbs, whereas those without *DFL16.1* could not. *DFL16.1* gene–deficient mice proved more susceptible to challenge with live *Streptococcus pneumoniae*. Our findings indicate that although production of self-reactive NAbs can be independent of germline D_H sequence, their capacity to provide protection against pathogens cannot. The potential relevance of these findings for the rational design of vaccines is discussed.

CORRESPONDENCE
Harry W. Schroeder Jr.:
hwsj@uab.edu

Abbreviations used: LDA, limiting dilution analysis; LDL, low-density lipoprotein; NAb, natural antibody; Nat-LDL, native LDL; OxLDL, oxidized LDL; PC, phosphorylcholine; PerC, peritoneal cavity; T15-Id, T15 idiotype.

Igs present in the sera of normal individuals in the absence of exogenous antigenic stimulation are termed natural antibodies (NAbs). The repertoire and reactivity pattern of NAbs are conserved both within and between species (Avrameas, 1991) and are remarkably stable. IgM is the dominant NAb isotype, and most, if not all, NAbs appear to be the products of B-1 B cells (Hayakawa et al., 1984, 1986a; Sidman et al., 1986; Haas et al., 2005; Baumgarth, 2011; Choi et al., 2012). The Igs produced by these lymphocytes often demonstrate decreased or absent N-region addition at the V-D and D-J junctions, emphasizing the major contribution of germline-encoded sequence to their specificity (Feeney, 1991; Tornberg and Holmberg, 1995; Kantor et al., 1997; Vale et al., 2010). NAbs are considered to constitute an innate component of the adaptive immune response, as they provide one of the first lines of defense against invading pathogens (Briles et al., 1981; Benedict and Kearney, 1999; Ochsenbein et al., 1999).

In mice, NAbs are present at equivalent levels in specific pathogen–, germ-, and even exogenous antigen–free animals, suggesting a role for endogenous ligands in the selection of the NAb repertoire (Bos et al., 1989; Haury et al., 1997). Accordingly, elegant experiments have shown that naturally generated B-1 B cells secreting antithymocyte NAb required the presence of the cognate endogenous antigen (Thy-1/CD90) for B cell expansion and serum autoantibody secretion (Hayakawa et al., 1999). Some NAbs also appear to play a role in normal cellular homeostasis, helping rid the body of cellular and molecular

The Rockefeller University Press $30.00
J. Exp. Med. 2013 Vol. 210 No. 5 875-890
www.jem.org/cgi/doi/10.1084/jem.20121861

The Journal of Experimental Medicine

debris (Aprahamian et al., 2004; Binder and Silverman, 2005; Kaveri et al., 2012). One classical example in mice of the dual role of NAbs involves the NAb response to endogenous oxidation-specific epitopes on oxidized low-density lipoprotein (LDL [OxLDL]) and apoptotic cells (Shaw et al., 2000; Binder et al., 2003; Binder and Silverman, 2005; Chen et al., 2009; Chou et al., 2009). In response to OxLDL, there appears to be selection and expansion of NAbs bearing the germline-encoded T15 idiotype (T15-Id) in the peripheral B cell repertoire (Shaw et al., 2000; Kearney, 2005). T15-Id$^+$ NAbs also bind to phosphorylcholine (PC) present on the cell wall of *Streptococcus pneumoniae* (Potter and Leon, 1968; Briles et al., 1981), constituting 60–80% of the natural anti-PC response (Gearhart et al., 1975; Sigal et al., 1975; Lévy, 1984; Feeney et al., 1988). Although many antibodies can bind PC, those containing the germline canonical T15-Id confer optimal protection against lethal *S. pneumoniae* bacteremia (McDaniel et al., 1984) and fatal sepsis (Briles et al., 1982) in mice, and low levels of IgM antibodies to PC have been recently associated with a higher risk of cardiovascular disease in humans (de Faire et al., 2010).

Although the key roles played by NAbs in host homeostasis and defense are increasingly appreciated, a major remaining question is the nature of the forces that shape the composition of the NAb repertoire. One thesis, which we may refer to as the natural selection hypothesis, holds that the germline composition of the NAb repertoire is critical for its dual function as a protector against both endogenous and exogenous antigens and thus has been naturally selected during evolution. The antithesis, which we may refer to as the self-antigen–driven or somatic selection hypothesis, proposes that exposure to self-antigen drives the production of dual-function NAbs irrespective of germline sequence.

The T15-Id is conserved across multiple mouse strains and is tightly associated with the use of a specific V_H (*V_HS107.1*) and a specific V_L (*V_κ22*; Crews et al., 1981). Disruption of the *V_HS107.1* gene results in an inability to mount a protective immune response to *S. pneumoniae* (Mi et al., 2000). In common with many other B-1a Igs, canonical anti-PC T15 CDR-H3s lack N-region addition and use their D_H, in this case *DFL16.1*, in only one of six potential reading frames, RF1 (Feeney, 1991). These findings raised the possibility that the complete germline sequence of DFL16.1 in general, and of RF1 in particular, would be critical for NAb protection against *S. pneumoniae*, with N addition playing a deleterious role (Benedict and Kearney, 1999). However, this presumed centrality of naturally selected *DFL16.1* germline sequence, either partial or in its entirety, in promoting production of NAb induced by endogenous OxLDL and in preventing potentially atherogenic uptake of this lipid has not been experimentally verified.

In this work, we report the use of a panel of BALB/c mice with altered D_H alleles (Schelonka et al., 2005, 2008; Ippolito et al., 2006; Zemlin et al., 2008) to both qualitatively and quantitatively test the relative roles of germline versus somatic selection of CDR-H3 sequence in the generation and function of the anti-OxLDL, anti-PC, and T15-Id$^+$ NAb repertoires. We present data that support the moderating concept that natural selection of conserved D (diversity) sequence and self-antigen–driven somatic selection operate in concert to create a protective, functional NAb repertoire reactive with a bacterial cell wall component. In remarkable contrast, NAb reactivity and function in the case of an endogenous antigen representative of molecular debris do not show this dependence on evolutionarily conserved D_H sequences.

RESULTS

Evidence for a conserved range of self-reactivities expressed by the NAb repertoire despite changes in its germline composition

We had previously used techniques of cre-loxP–based gene targeting on a BALB/c embryonic stem cell line to delete 12 of the 13 D_H gene segments in the D_H locus, retaining only the single *DFL16.1* segment (*ΔD-DFL* mice). We then generated a panel of D_H-altered mice by replacing the single *DFL16.1* segment with a twice-frameshifted *DFL16.1* gene segment (*ΔD-DμFS*) or an inverted *DSP2.2* gene segment (*ΔD-iD*; Schelonka et al., 2005, 2008; Ippolito et al., 2006; Zemlin et al., 2008; Schroeder et al., 2010).

To gain insight into the role played by germline D_H sequence in the antigen specificity of the NAb repertoire, we performed a semiquantitative immunoblot assay that enables an en bloc analysis of the self-reactivity of IgM present in the serum of unmanipulated WT and the D_H-altered mutant mice (Nobrega et al., 1993; Haury et al., 1994; Mouthon et al., 1995). Sera were tested for reactivity to self-proteins isolated from brain, muscle, heart, and liver (Fig. S1 A and not depicted). The serum IgM self-reactivity pattern (actual repertoire) was remarkably well-conserved in mice that generate very different primary CDR-H3 repertoires at multiple stages and subsets of B cell development, including the B-1 compartments (unpublished data). To test whether the self-reactivity pattern observed in serum is also conserved at the cellular level (available repertoire), we sorted and cultured peritoneal cavity (PerC) B-1a, B-1b, and B-2 cells under mitogen stimulation to induce polyclonal IgM secretion and tested the supernatants using the immunoblot assay. Whereas the self-reactivity profiles from B-1a culture supernatants were highly conserved among the different mouse strains, reflecting those observed in the serum, there was less conservation in B-1b and still less in the B-2 cell culture supernatants (Fig. S1 B). These results suggest that the self-reactivity profile of the serum NAb repertoire is conserved and is essentially independent of germline D_H sequence.

Serum levels and potential physiological function of anti-OxLDL NAbs are maintained despite limitation and alterations of D_H genes

The remarkable conservation of NAb self-reactivities observed in the en bloc immunoblot assay could also suggest conservation of function. To test both the reactivity and function of the NAb produced by these gene-altered mice, we turned to

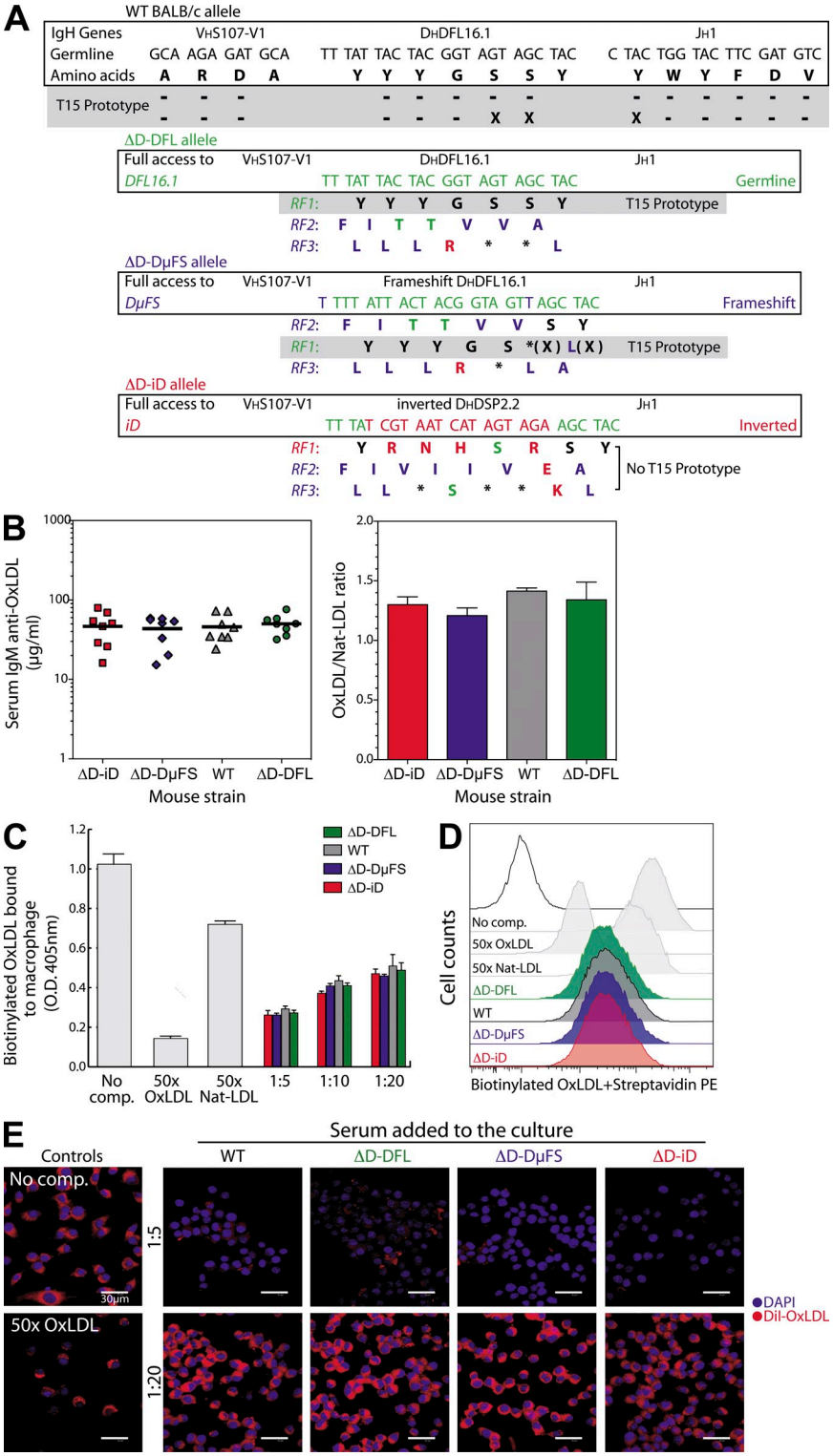

Figure 1. The serum levels and potential functionality of anti-OxLDL IgM NAbs are unaffected by changes in the germline sequence of the D_H locus. (A) Schematic representation of the BALB/c WT D_H and D_H-altered loci in the context of T15 prototypic sequences. (top) Amino acid sequence of the prototypic T15 CDR-H3 (Feeney, 1991) compared with the germline sequences of *V_HS107.1*, *D_HDFL16.1*, and *J_H1*; "-" indicates identical amino acid usage, and "X" indicates alternative amino acid usage. Amino acid sequences were encoded by each D_H-altered allele in the three direct RFs: *ΔD-DFL* (upper middle), *ΔD-DμFS* (lower middle), and *ΔD-iD* allele (bottom). Neutral, hydrophobic, and charged amino acids are shown in green, blue, and red, respectively; asterisks indicate termination codons. (B) Levels of serum anti-OxLDL IgM in WT and D_H-altered naive mice. (left) Levels of IgM antibodies are shown as an equivalent titer (μg/ml) to the BALB/c IgM anti-PC–producing hybridoma BH8 (Kearney et al., 1981). The horizontal lines indicate the mean value of each group. (right) Anti-OxLDL IgM levels expressed as ratios between anti-OxLDL and anti-Nat-LDL in absorbance units. (C) Immunoenzymatic analysis of inhibition of Biot-OxLDL binding to RAW 264.7 macrophages. RAW 264.7 macrophages were incubated with Biot-OxLDL in the presence of 1:5, 1:10, and 1:20 diluted pooled sera from each mouse strain. The extent of OxLDL binding is expressed as optical density. (B and C) Error bars indicate SD of the mean. (D) Representative flow cytometric analysis of inhibition of Biot-OxLDL binding to RAW 264.7 macrophages. Cells were incubated in the absence (dark line) or presence of Biot-OxLDL. RAW 264.7 macrophages were incubated with Biot-OxLDL in the presence of 1:5, 1:10 (shown), and 1:20 diluted pooled sera from each mouse strain. The extent of OxLDL binding is expressed as the intensity of PE fluorescence. (E) Representative confocal microscopy images of inhibition of DiI-OxLDL binding/uptake to RAW 264.7 macrophages. RAW 264.7 macrophages were incubated with DiI-OxLDL in the presence of 1:5 (shown), 1:10, and 1:20 (shown) diluted pooled sera from each mouse strain. The extent of OxLDL binding/uptake was examined with a 63× oil immersion objective using a 546-nm filter set. In each assay, the specific binding of Biot-OxLDL or DiI-OxLDL to the macrophages was shown by incubation in the absence (No comp.) and presence of 50-fold excess of unconjugated OxLDL or Nat-LDL. Each assay was performed in at least two independent experiments, and one representative dataset is shown. Bars, 30 μm.

the well-defined T15 system. Essentially two CDR-H3 T15 prototypes are generated by the IgH allele of BALB/c WT mice, the dominant one entirely encoded by the germline V_H, J_H, and D_H *DFL16.1* RF1 gene segment sequence (Fig. 1 A, top; Feeney, 1991). Our panel of mice provided us with a suitable range of alternative D_H sequences to study the relationship between naturally selected, germline D_H amino acid sequence, both for self-reactivity and for protection against a common exogenous pathogen (for further details see Fig. 1 A and Materials and methods).

In unmanipulated mice, we found that consistent with our en bloc analysis, the physiological levels of anti-OxLDL NAbs

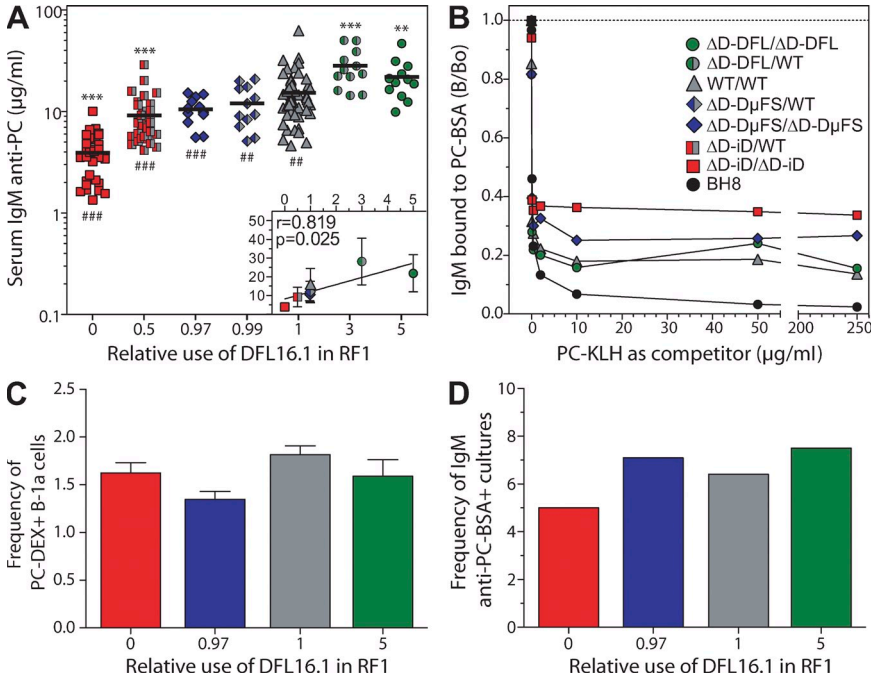

Figure 2. Loss of evolutionary conserved D_H sequence quantitatively decreases the serum levels of anti-PC NAbs but not the frequency of anti-PC B-1a precursors. (A) Levels of serum natural anti-PC IgM in WT and D_H-altered naive mice as a function of the relative use of *DFL16.1* in RF1 (*R* value). The data are combined from three independent experiments. The *R* value was calculated as shown in Table 1 and detailed in Materials and methods. The horizontal lines indicate the mean value of each group. Significantly different from WT: **, $P \leq 0.01$; ***, $P \leq 0.001$. Significantly different from *ΔD-DFL*: ##, $P \leq 0.01$; ###, $P \leq 0.001$. (inset plot) Mean serum concentrations (±SD) of anti-PC from each mouse strain are presented as a function of *R* value. A regression line is plotted. The strength of the relationship between antibody production and *R* value was calculated and is given in each panel as *r*, Pearson's correlation coefficient, and the p-value of the analysis. Levels of IgM antibodies are shown as an equivalent titer (μg/ml) to the BALB/c IgM anti-PC–producing hybridoma BH8 (Kearney et al., 1981). (B) A constant amount of pooled sera from WT and D_H-altered naive mice was incubated with PC-BSA in the absence or presence of increasing amounts of PC-KLH. At least five sera samples were included in each pool. Data are the mean of triplicate determinations expressed as ratio of IgM binding to PC-BSA in the presence (B) or absence (B_0) of competitor (B/B_0). (C) Frequency of PerC B-1a cells bearing IgM anti-PC estimated by flow cytometry. Histogram bars show the mean percentage of B-1a IgM^+ $PC\text{-}DEX^+$ from each mouse strain. At least four mice per group were used for each independent experiment. Error bars indicate SD of the mean. (D) PerC B-1a cells were sorted, and variable numbers of cells were cultured under polyclonal stimulation for IgM secretion. The frequency of B-1a cells secreting IgM anti-PC in vitro was estimated by LDA. Histogram bars show the frequency, calculated by the Poisson distribution, of culture supernatants containing anti-PC IgM. Experiments displayed in B–D were performed at least twice.

were indistinguishable among the different strains, irrespective of the availability of evolutionarily conserved *DFL16.1* gene segment sequence (Fig. 1 B). To test the antiatherogenic potential of anti-OxLDL NAbs generated under varying levels of *DFL16.1* availability, we then used immunoenzymatic (Fig. 1 C), flow cytometry (Fig. 1 D), and confocal microscopy (Fig. 1 E) assays to evaluate the capacity of sera from each mouse strain to inhibit binding/uptake of OxLDL to macrophages. In each case, we found that pooled serum from each D_H-altered mouse strain was equally efficacious to WT in blocking binding of OxLDL to macrophages. Collectively, these results suggested that both anti-OxLDL NAb serum levels and functionality had apparently been both qualitatively and quantitatively unaffected by the enhancement, alteration, or complete elimination of germline *DFL16.1* gene segment sequence usage.

Loss of the DFL16.1 gene sequence decreases the physiological levels of serum anti-PC antibodies

We then tested whether the production of anti-PC NAbs had been influenced by altering D_H. We first measured the levels of anti-PC antibodies in the serum of naive mice (Fig. 2 A). To perform quantitative calculations for this analysis, we used a parameter that we term *R* value (Table 1; for further details see Materials and methods), which is an expression of the likelihood of the use of the *DFL16.1* RF1 sequence. We related the *R* value to the prevalence of anti-PC antibodies bearing the T15-Id. Among the seven homozygous and heterozygous genotypes of mice examined (Table 1), the titer of anti-PC NAbs was lowest in the complete absence of *DFL16.1* (homozygous *ΔD-iD* mice, $P < 0.001$ and $P < 0.001$ versus both WT and *ΔD-DFL*, respectively), followed by the heterozygous WT/*ΔD-iD* (Fig. 2 A). Anti-PC production in both heterozygous and homozygous *ΔD-DμFS* mice, which retained the *DFL16.1* core sequence, was lower than WT but not significantly so. However, anti-PC production proved highest in the heterozygous *ΔD-DFL*/WT mice, followed by the homozygous *ΔD-DFL* mice ($P < 0.001$ and $P < 0.01$, respectively, when compared with WT). Evaluation of the anti-PC titer as a potential function of the use of *DFL16.1* in RF1 relative to the WT (*R* value) revealed a strong, positive correlation ($r = 0.82$; $P = 0.02$; Fig. 2 A, inset). Competition assays showed that the binding of serum IgM from each of the mouse strains to PC-BSA was significantly inhibited by PC-KLH (at least 60%), indicating that most of the natural IgM bound specifically to PC and not to the carrier link (Fig. 2 B). These data suggested that, contrary to what was observed for anti-OxLDL NAbs, the availability of B cells incorporating germline-encoded *DFL16.1* RF1 sequence into their Ig H chains might directly influence the physiological production of anti-PC NAbs.

Table 1. Calculation of the use of DFL16.1 in RF1 relative to the WT mice

Genotype (alleles A/B)	Allele A			Allele B			*R* value
	R1	R2	R3	R1	R2	R3	
ΔD-DFL/ΔD-DFL[a]	1	5	1	1	5	1	5
ΔD-DFL/WT	1	5	1	1	1	1	3
WT/WT	1	1	1	1	1	1	1
ΔD-DμFS/WT	0.59	5	0.33	1	1	1	0.99
ΔD-DμFS/ΔD-DμFS[b]	0.59	5	0.33	0.59	5	0.33	0.97
ΔD-iD/WT	0.48	0	1	1	1	1	0.5
ΔD-iD/ΔD-iD[c]	0.48	0	1	0.48	0	1	0

R1 is the proportion of mature recirculating IgM$^+$ IgD$^+$ B cells in the bone marrow relative to WT. R2 is the expected frequency of *DFL16.1* gene usage relative to WT. R3 is the expected frequency of RF1 usage relative to WT. The formula used to calculate the *R* value is $[R_{\text{allele A}}\ (R1 \times R2 \times R3) + R_{\text{allele B}}\ (R1 \times R2 \times R3)] \times 0.5$.
[a]The data used to calculate the R1, R2, and R3 values were retrieved from Schelonka et al. (2005).
[b]The data used to calculate the R1, R2, and R3 values were retrieved from Schelonka et al. (2008) and Zemlin et al. (2008).
[c]The data used to calculate the R1, R2, and R3 values were retrieved from Ippolito et al. (2006).

Frequency of potential anti-PC precursors is not obviously altered by availability of the germline *DFL16.1* gene segment

We next tested whether these serum NAb alterations reflected differences in the frequency of anti-PC B cell clones, focusing on the PerC B-1a population. We observed that the germline composition of the D_H locus had little, if any, effect in determining the frequency of B-1a cells in the PerC-bearing BCRs with anti-PC reactivity (Fig. 2 C), as analyzed by flow cytometry. To further confirm our finding that PC-specific B cell frequencies were unaffected by *DFL16.1* sequence alteration or loss, we tested the capacity of individual B cells to secrete anti-PC antibody in vitro. Limiting dilution analysis (LDA) showed no significant correlation between *R* and the frequency of B-1a clones secreting anti-PC IgM, confirming the results of flow cytometric analysis (Fig. 2 D). Thus, in contrast to the D_H sequence–associated variation in the serum levels of the anti-PC NAbs (actual anti-PC repertoire), the prevalence of PerC B-1a cells with the potential to secrete anti-PC antibodies (available anti-PC repertoire) did not appear to be affected by changes in or loss of *DFL16.1* germline sequence content.

Availability of germline *DFL16.1* gene sequence quantitatively controls both the serum levels and the frequency of B-1a cells producing anti-PC T15-Id$^+$ antibodies

In BALB/c WT mice, 60–80% of anti-PC antibodies have been reported to be T15-Id$^+$ (Sigal et al., 1977; Feeney et al., 1988). We thus postulated that the decrease in the serum levels of anti-PC NAbs observed in mice either lacking *DFL16.1* entirely or possessing an altered *DFL16.1* sequence would be accompanied by a decrease in serum T15-Id$^+$ NAb levels. Using the T15 clone–specific antibody (AB1.2), we found that the titer of T15-Id$^+$ antibodies in the homozygous *ΔD-iD* mice was at least one log lower than that of the other six genotypes ($P < 0.05$ for both the WT and *ΔD-DFL* mice; Fig. 3 A). When compared with homozygous *ΔD-DFL* mice, T15-Id$^+$ antibodies were also less common in both heterozygous WT/*ΔD-iD* mice ($P < 0.05$) and homozygous *ΔD-DμFS* mice ($P < 0.05$). As observed in the total anti-PC serum levels, there was a strong positive correlation between T15-Id$^+$ levels and the *R* value ($r = 0.80$; $P = 0.03$; Fig. 3 A, inset). To independently estimate the levels of antibodies that express V_H-T15 (*V_HS107.1*) and V_L-T15 (*V_κ22*), we used two additional antibodies, designated TC68 and TC139, respectively. Although the serum levels of antibodies using the *V_HS107.1* heavy chain gene were significantly lower in the mice using the *ΔD-iD* allele when compared with WT or mice using the *ΔD-DFL* allele, we did not observe a positive correlation with *R* (Fig. 3 B). In contrast, the prevalence of *V_κ22* light chain–containing serum antibodies in the seven genotypes roughly followed the same pattern observed in anti-PC antibody reactivity (Fig. 3 C), with a high degree of correlation between *V_κ22* prevalence and *R* ($r = 0.78$; $P < 0.04$; Fig. 3 C, inset). A competition assay using AB1.2 as a competitor showed 55%, 70%, and 80% inhibition of IgM binding to PC-BSA in *ΔD-DμFS*, WT, and *ΔD-DFL* homozygous mice, respectively. No significant inhibition was observed in pooled *ΔD-iD* sera, suggesting that the low level of T15-Id$^+$ reactivity in these mice reflected binding to noncanonical T15-V_H– and/or T15-V_L–containing antibodies, perhaps caused by weakly cross-reactive determinants (Fig. 3 D). These data suggest that the availability of germline-encoded *DFL16.1* gene segment sequence quantitatively determines the physiological production of anti-PC antibodies through the control of T15-Id$^+$ expression.

By FACS and LDA, we then analyzed the frequency of B-1a cells in the PerC bearing anti-PC T15-Id$^+$ IgM. Contrary to the relatively stable numbers of B-1a cells bearing anti-PC BCRs, the frequency of T15-Id$^+$ B-1a cells directly correlated with the *R* value, thus reflecting the availability of germline *DFL16.1* gene segment sequence in RF1 (Fig. 3, E and F). These data support the view that the potential to secrete T15-Id$^+$ antibodies is also qualitatively dependent on the germline sequence of the D_H locus.

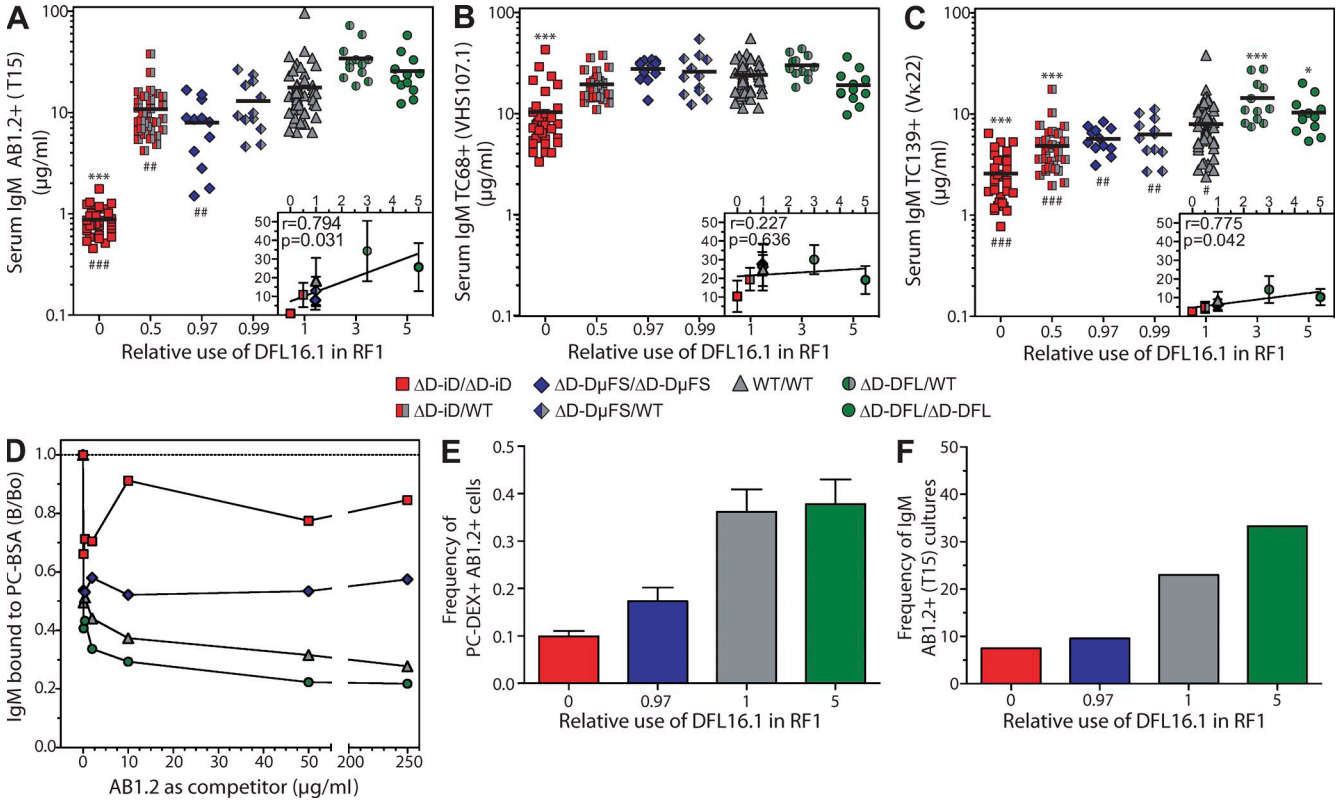

Figure 3. Loss of *DFL16.1* RF1 sequence quantitatively controls both the serum levels of T15-Id$^+$ NAbs and the frequency of anti-PC T15-Id$^+$ B-1a cells. (A–C) Levels of serum IgM expressing the T15-Id$^+$ (A), IgM antibodies dependent on the use of the heavy chain $V_HS107.1$ gene segments, TC68$^+$ (B), and IgM antibodies dependent on the use of the light chain $V_κ22$ gene segments, TC139$^+$ (C), in WT and D_H-altered naive mice as a function of the relative use of *DFL16.1* in RF1 (*R* value). The data are combined from three independent experiments. The horizontal lines indicate the mean value of each group. (inset plots) Mean serum concentrations (±SD) of IgM T15-Id$^+$, TC68$^+$, or TC139$^+$ from each mouse strain are presented as a function of *R* value. Significantly different from WT: *, $P \le 0.05$; ***, $P \le 0.001$. Significantly different from *ΔD-DFL*: #, $P \le 0.05$; ##, $P \le 0.01$; ###, $P \le 0.001$. Levels of IgM antibodies are shown as an equivalent titer (μg/ml) to the BALB/c IgM anti-PC–producing hybridoma BH8 (Kearney et al., 1981). (D) A constant amount of pooled sera from WT and D_H-altered naive mice was incubated with PC-BSA in the absence or presence of increasing amounts of monoclonal AB1.2 anti–T15-Id antibody. At least five sera samples were included in each pool. Data are the mean of triplicate determinations expressed as the ratio of IgM binding to PC-BSA in the presence (B) or absence (B_0) of competitor (B/B_0). (E) Frequency of PerC B-1a cells bearing IgM anti-PC T15-Id$^+$ estimated by flow cytometry. Histogram bars show the mean percentage of B-1a PC-DEX$^+$ AB1.2$^+$ from WT and D_H-altered naive mice. At least four mice per group were used for each independent experiment. Error bars indicate SD of the mean. (F) Frequency of sorted peritoneal B-1a cells secreting IgM T15-Id$^+$ in vitro, as estimated by LDA. Histogram bars show the frequency of culture supernatants containing AB1.2$^+$ IgM from each mouse strain. Experiments displayed in D–F were performed at least twice.

The frequency of transcripts encoding the classical T15 CDR-H3 amino acid sequence in the anti-PC B-1a precursors is directly proportional to the availability of the *DFL16.1* RF1 sequence

We next examined at the amino acid level the actual composition of the PC-specific Ig heavy chain repertoire in B-1a cells from mice with varying access to *DFL16.1* RF1 sequence. From the PerC of homozygous D_H-altered and WT mice, we sorted PC-DEX$^+$ AB1.2$^+$ B-1a cells and sequenced their CDR-H3 (Fig. 4 A). The classical T15 CDR-H3 amino acid sequence was found only in the B-1a cell population that stained highly for PC-DEX and AB1.2 (Fig. 4 A and Table S1). This is consistent with observations by Dizon and Kearney, showing by flow cytometry that only the PC-DEX^{hi} B cell population is inhibitable using PC-BSA as a blocking reagent (unpublished data). Indeed, we found that the T15 heavy chain prototype was found only in B-1a cells derived from mice that carry the *DFL16.1* gene segment sequence in proportions dependent on its availability for usage, i.e., 70%, 25%, and ∼4% in *ΔD-DFL*, WT, and *ΔD-DμFS* mice, respectively (Fig. 4 B). Strikingly, both the prevalence of N addition and the diversity of V_H/J_H usage increased as the complete sequence of *DFL16.1* in RF1 became less available to the D_H-altered mice (Fig. 4 B and Table S1).

N addition can be used to recreate the canonical T15 CDR-H3 amino acid sequence if partial *DFL16.1* RF1 sequence is available

Detailed analysis of the CDR-H3 sequence in transcripts from B-1a cells revealed that junctional diversity, including N-region addition and nucleotide nibbling, can rescue the canonical V_H-T15 sequences in mice forced to use the frameshifted

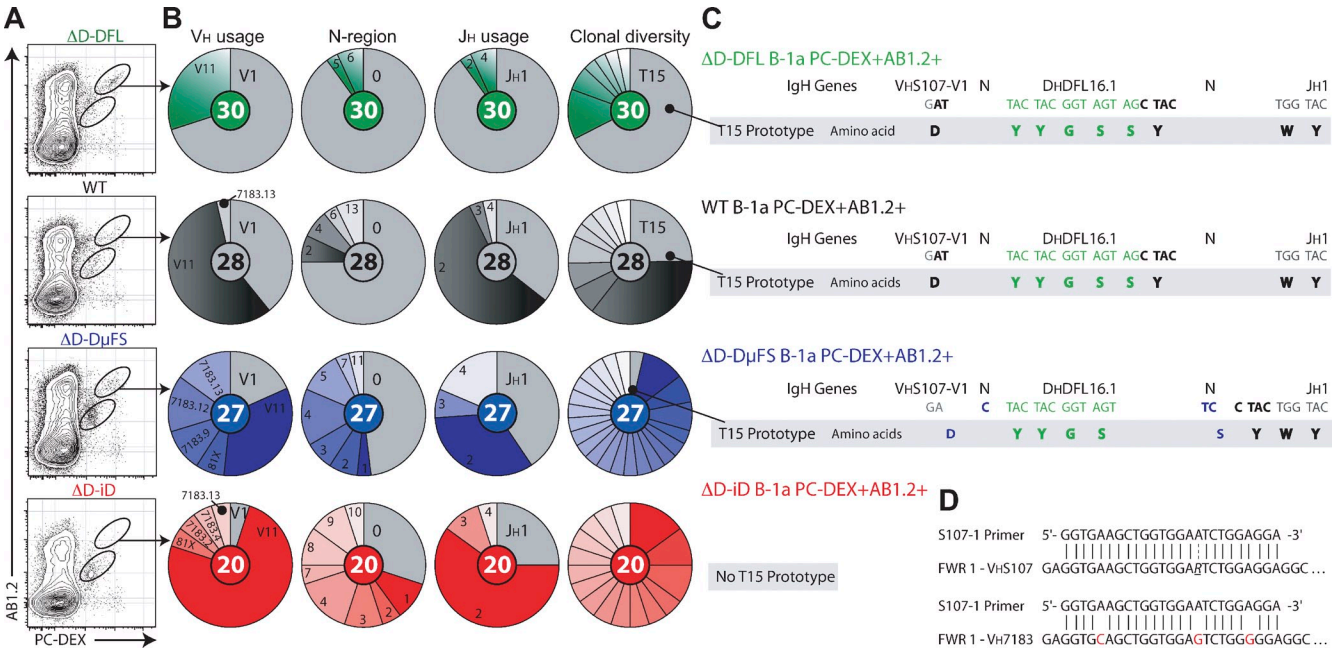

Figure 4. Junctional diversity rescues the T15-Id in mice forced to use the frameshifted *DFL16.1* gene segment. (A) Flow cytometry plots show representative gates used to sort peritoneal B-1a cells that stain highly for PC-DEX and AB1.2 from each mouse strain. Peritoneal B-1a cells were sorted from at least five mice per group to achieve sufficient numbers of cells for RNA extraction and sequencing. (B) CDR-H3 analysis of transcripts of sorted PC-DEX^{hi} AB1.2^{+} B-1a cells from each mouse strain. V_H usage, pie charts depict the proportion of V_H gene usage. N-region, pie charts depict the proportion of N-region addition distributed by the number of N nucleotides added at both junctions. The numbers represent the amount of N nucleotides added at both junctions. J_H usage, pie charts depict the proportion of J_H element usage. The numbers represent the J_H gene segment. Clonal diversity, pie charts depict the proportion of individual sequences, and the prototypic T15 is in gray (see Fig. 1 A and Table S1). (C) CDR-H3 nucleotide and amino acid sequences found in the T15 prototypes in each mouse strain. The V-D and D-J overlap sequences are represented in bold, the *DFL16.1* canonical sequences in green, and N-region addition in blue. (D) Shown are the S107-1 primer sequence homologies with *V_HS107* family and with members of the *V_H7183* family (Feeney, 1990). A red letter indicates a mismatch between the S107-1 primer and the V_H7183 consensus sequence.

DFL16.1 gene segment (*ΔD-DμFS*), which preferentially encodes hydrophobic sequences in place of the neutral T15 amino acid sequence. Extensive nucleotide nibbling at the 3′ end of the D_H segment eliminated the D/J microhomology that otherwise would have helped guide D→J rearrangement into the frameshifted RF2 as well as the stop codon near the 3′ terminus of RF1 created by the *DμFS* frameshift (Fig. 4 C). N addition at both the V-D and D-J junctions then created a complete, canonical CDR-H3 T15 amino acid sequence. Although in this case the data suggest that somatic selection, perhaps driven by endogenous antigen, can rescue and expand rare TdT-dependent T15 B cell clones, the low frequency observed suggests that the power of N addition to create the T15-Id is limited and dependent on the availability of at least partial *DFL16.1* germline RF1 sequence because we were unable to detect the presence of such N nucleotide–generated T15 B cell clones in the *ΔD-iD* mice.

Loss of the evolutionary conserved D_H sequence severs the link between anti-PC and anti-OxLDL reactivities

To gain insight into the quality of serum anti-PC antibodies from mice with varying access to *DFL16.1* RF1 sequence, we determined the levels of NAb cross-reactivity to OxLDL and PC-BSA, as well as to binding by anti–T15-Id antibodies. Competition immunoassay studies indicated that the binding of natural serum IgM to OxLDL was inhibited by PC-BSA in a manner that was proportional to the relative use of the *DFL16.1* RF1 sequence (Fig. 5 A). In particular, PC-BSA completely failed to inhibit the binding of IgM from the pooled sera of *ΔD-iD* mice to OxLDL (Fig. 5 A). The T15-Id–specific antibody, AB1.2, was able to inhibit only a fraction of IgM binding to OxLDL in serum from *ΔD-DFL* and WT mice (Fig. 5 B). These findings were also replicated using OxLDL as a competitive inhibitor of binding to PC-BSA (Fig. 5 C). These data are in agreement with the observation that a major fraction of anti-PC antibodies, a significant proportion of which are T15-Id^{+}, can be physiologically generated in the presence of germline-encoded *DFL16.1* sequence and cross-react with the endogenous antigen OxLDL (Shaw et al., 2000). However, our data go beyond these previous studies to strongly suggest that although anti-PC NAbs are still generated in the absence of germline *DFL16.1* sequence (e.g., in the *ΔD-iD* homozygous mice), these NAbs do not cross-react with the phospholipid-related epitope on OxLDL. Collectively, these results indicate that the elimination of germline *DFL16.1* sequence has severed the relationship between self-antigen–driven, antiatherogenic OxLDL NAb and anti-PC NAb production.

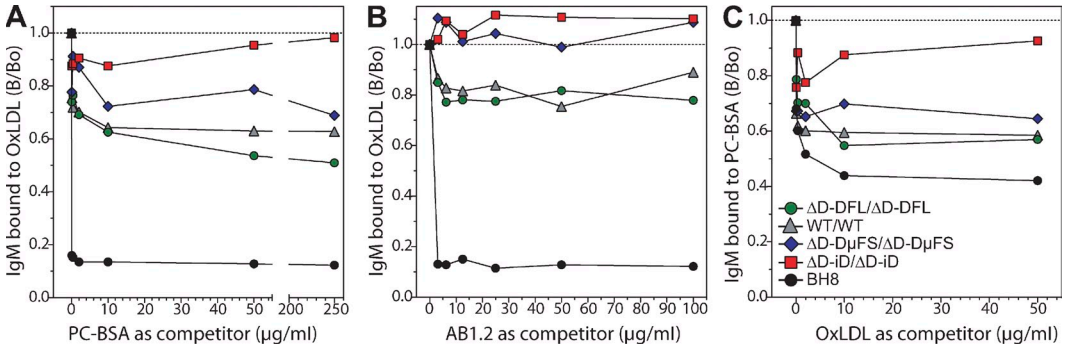

Figure 5. Loss of the canonical *DFL16.1* gene segment quantitatively severs NAb cross-reactivity between anti-PC and OxLDL. (A and B) A constant amount of pooled sera from WT and D_H-altered naive mice was incubated with OxLDL in the presence of increasing amounts of PC-BSA (A) and monoclonal AB1.2 anti–T15-Id antibody (B). Data are the mean of triplicate determinations expressed as ratio of IgM binding to OxLDL in the presence (B) or absence (B_0) of competitor (B/B_0). (C) A constant amount of pooled sera from WT and D_H-altered naive mice was incubated with PC-BSA in the presence of increasing amounts of OxLDL. At least five sera samples were included in each pool. At least two independent experiments were performed.

Immunization with heat-inactivated *S. pneumoniae* recovers the anti-PC but not the T15-Id$^+$ response in mice lacking the *DFL16.1* gene segment

Although the levels and quality of the anti-PC NAb were significantly affected by the availability of *DFL16.1* gene segment sequence, the frequencies of PerC B-1a anti-PC clones were not. We thus tested the ability of the D_H-altered mice to produce anti-PC antibodies after exogenous stimulation. The levels of anti-PC and the T15 components (T15-Id, $V_HS107.1$, and $V_\kappa 22$) in the sera of each mouse strain were measured 7 d after immunization with heat-inactivated *S. pneumoniae*. Differing from the pattern observed in naive mice, anti-PC production in immunized homozygous *ΔD-iD* mice proved similar to that observed in WT and *ΔD-DFL* mice (Fig. 6 A). Thus, the link between *R* and anti-PC titers had also been severed (Fig. 6 A, inset).

Importantly, the production of anti-PC antibodies was similar among six of the seven genotypes, but the production of T15-Id$^+$ antibodies proved to be strongly influenced by the composition of the D_H locus (Fig. 6 B). A strong correlation between *R* and the T15-Id titer was observed (r = 0.82; P = 0.02; Fig. 6 B, inset). In particular, homozygous *ΔD-iD* mice demonstrated significant difficulty generating T15-Id$^+$ antibodies ($P < 0.05$ vs. WT and homozygous *ΔD-DFL*) even after antigen challenge. The levels of IgM antibodies using the V_HS107.1 were similar among homozygous *ΔD-iD*, WT, and *ΔD-DFL* mice after immunization (Fig. 6 C), and the correlation between *R* and the use of $V_HS107.1$ was extremely weak at best (r = 0.75; P = 0.068; Fig. 6 C, inset). However, as was the case in naive mice, the prevalence of serum antibodies containing the $V_\kappa 22$ light chain in the seven genotypes was comparable with that observed in antibodies with anti-PC reactivity (Fig. 2, A and D; and Fig. 6, A and D). The production of $V_\kappa 22$-bearing antibodies was significantly higher than WT in both *ΔD-iD* ($P < 0.001$) and *ΔD-DFL* homozygous mice ($P < 0.001$) and significantly lower in heterozygous *ΔD-iD* mice ($P < 0.001$). Caused in part by the markedly higher titer of IgM antibodies containing $V_\kappa 22$ light chain in homozygous *ΔD-iD* mice, there was no correlation between *R* and $V_\kappa 22$ usage (r = 0.23; P = 0.62; Fig. 6 D, inset). These data show that immunization promotes a serum anti-PC response even when germline-encoded *DFL16.1* gene sequence is not available, further confirming that the potential to secrete anti-PC antibodies is intact in all D_H-altered mouse strains, as was also observed after polyclonal stimulation in the LDA (Fig. 2 D).

Availability of evolutionarily conserved *DFL16.1* RF1 amino acid sequence is a critical factor for survival against challenge with live *S. pneumoniae*

The serum level of anti-PC antibodies in *ΔD-iD* mice after immunization with heat-inactivated bacteria proved indistinguishable from WT (Fig. 6 A), raising the question of whether the anti-PC antibody repertoire created in the complete absence of *DFL16.1* RF1 sequence (see Fig. 5 B), but with full access to $V_HS107.1$, J_H1, $V_\kappa 22$, and $J_\kappa 5$, would be able to protect against experimental infection with live *S pneumoniae*. We thus challenged cohorts of homo- and heterozygous *ΔD-iD* and WT mice with live *S. pneumoniae*. 7 d after challenge, survival of the WT (15 of 21) and heterozygous *ΔD-iD* mice (15 of 21) was significantly greater than that of the homozygous *ΔD-iD* mice (5 of 21; $P < 0.001$; Fig. 7 A). To assess whether the *ΔD-iD* mice that survived challenge with live *S. pneumoniae* had managed to produce levels of anti-PC and the protective T15 antibodies equivalent to WT or heterozygous control, the serum concentration of PC-binding antibodies and the titers of antibodies in the sera that expressed the T15-Id, $V_HS107.1$, or $V_\kappa 22$ markers were then measured in blood samples obtained from the survivor mice (Fig. 7 B).

Although the majority of *ΔD-iD* mice died from the infection, anti-PC production in the surviving homozygous *ΔD-iD* mice matched that observed in surviving WT or heterozygous *ΔD-iD* mice. However, the variance was pronounced within the homozygous *ΔD-iD* serum samples (Fig. 7 B), and a correlation between *R* and anti-PC serum levels was not observed (r = 0.95; P = 0.20; Fig. 7 B, inset). Serum levels of

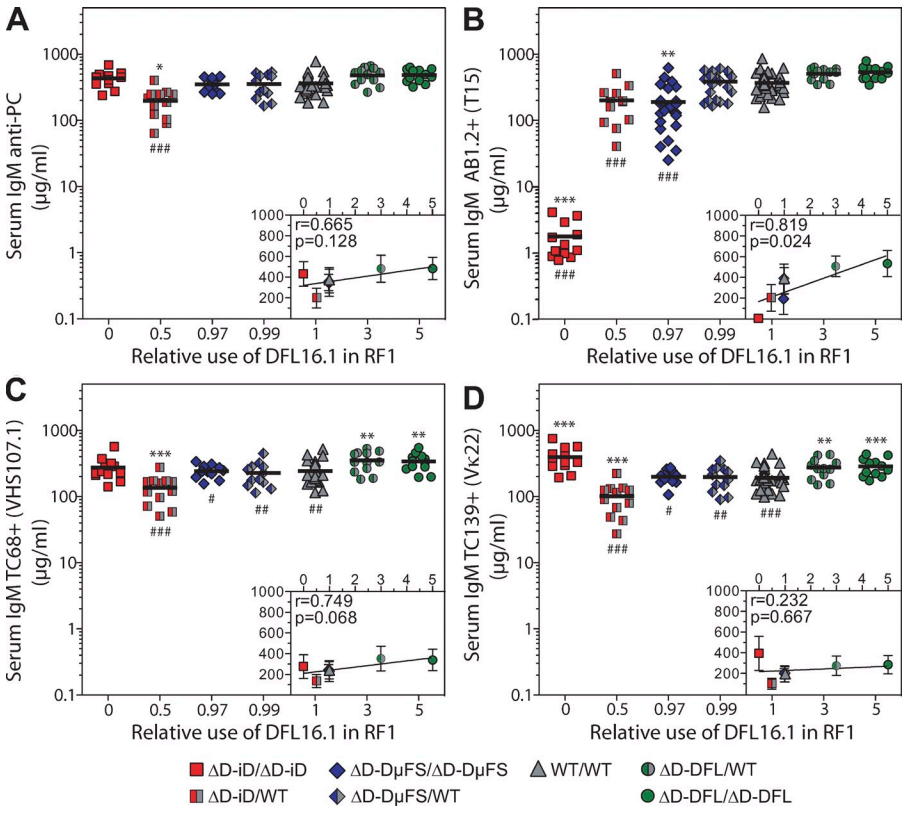

Figure 6. Immunization with heat-inactivated *S. pneumoniae* recovers the anti-PC response but not the T15-Id$^+$ in mice lacking the *DFL16.1* gene. WT, as well as homozygous and heterozygous for each D_H-altered mouse strain, mice were immunized i.v. with heat-inactivated *S. pneumoniae* (strain R36A), and serum was collected 7 d after immunization to measure the antibody levels. (A–D) Levels of serum IgM anti-PC (A), IgM expressing the T15-Id$^+$ (B), IgM antibodies dependent on the use of the heavy chain *V_HS107.1* gene segments, TC68$^+$ (C), and IgM antibodies dependent on the use of the light chain *V_κ22* gene segments, TC139$^+$ (D), in WT and D_H-altered mice 7 d after challenge with heat-inactivated *S. pneumoniae* (strain R36A). The levels of IgM antibodies for each mouse strain are plotted as a function of the relative use of *DFL16.1* in RF1 (*R* value). Levels of IgM antibodies are shown as an equivalent titer (µg/ml) to the BALB/c IgM anti-PC–producing hybridoma BH8 (Kearney et al., 1981). The data were combined from at least two independent experiments. The horizontal lines indicate the mean value of each group. Mean serum concentrations (±SD) of IgM anti-PC, T15-Id$^+$, TC68$^+$, or TC139$^+$ from each mouse strain are presented as a function of *R* value. Significantly different from WT: *, $P \le 0.05$; **, $P \le 0.01$; ***, $P \le 0.001$. Significantly different from *ΔD-DFL*: #, $P \le 0.05$; ##, $P \le 0.01$; ###, $P \le 0.001$.

antibodies bearing the T15-Id in the surviving homozygous *ΔD-iD* mice remained at baseline and were significantly decreased when compared with WT or heterozygous *ΔD-iD* littermate survivors ($P < 0.001$; Fig. 7 C). The correlation between *R* value and T15 serum concentration did not achieve statistical significance ($r = 0.99$; $P = 0.06$; Fig. 7 C, inset). The prevalence of antibodies using *V_HS107.1* was the same among all the survivors irrespective of genotype (Fig. 7 D), and no significant correlation between *R* and *V_HS107.1* prevalence ($r = 0.83$; $P = 0.38$; Fig. 7 D, inset) was observed. The prevalence of antibodies using *V_κ22* was again the same among all the survivors irrespective of genotype (Fig. 7 E), and again no correlation between R and *V_κ22* prevalence ($r = 0.98$; $P = 0.13$; Fig. 7 E, inset) was observed.

DISCUSSION

Using genetically manipulated mice, we have previously shown the importance of conserved D_H gene sequence content in delimiting the composition of the CDR-H3 repertoire (Schroeder et al., 2010). However, constraints in the CDR-H3 repertoire were also observed in unmanipulated WT mice (Ivanov et al., 2005; Schelonka et al., 2007; Vale et al., 2010), suggesting a role for naturally selected D_H genes in defining the composition of the NAb repertoire and, by doing so, potentially regulating NAb functions. The key roles played by NAbs in host defense have been extensively documented (Briles et al., 1981; Benedict and Kearney, 1999; Ochsenbein et al., 1999; Zhou et al., 2007; Rapaka et al., 2010), and more recently their roles in tissue homeostasis have become increasingly appreciated (Shaw et al., 2000; Binder et al., 2003; Chen et al., 2009; Kyaw et al., 2011; Kaveri et al., 2012). Nevertheless, major questions regarding the forces that shape the NAb repertoire remain unanswered. In this study we tested two, in many ways competing, hypotheses: first, that the germline composition of the NAb repertoire is critical for its dual function as a protector against both endogenous and exogenous antigens and, second, that exposure to self-antigen drives the production of these functional NAbs irrespective of germline sequence. Although these hypotheses are not mutually exclusive, they imply major differences regarding the forces that underlie the generation of the NAb repertoire, and the predominance of one upon the other would have distinct functional consequences.

We found that serum IgM NAb from D_H-altered mice have reactivity patterns that are predominantly focused on the same self-antigens that dominate the NAb repertoire in WT animals (Fig. S1 A). These data not only reinforce the view that self-antigens drive the production of NAb reactivities, as previously shown by Hayakawa et al. (1999), but also suggest that this property of NAb elicitation is preferentially driven by a delimited subset of the self-antigens (Mouthon et al., 1995).

It is well established that antigen-binding specificity does not always correlate with antibody function (Bachmann et al., 1997); therefore, the study of the well-defined T15 system as

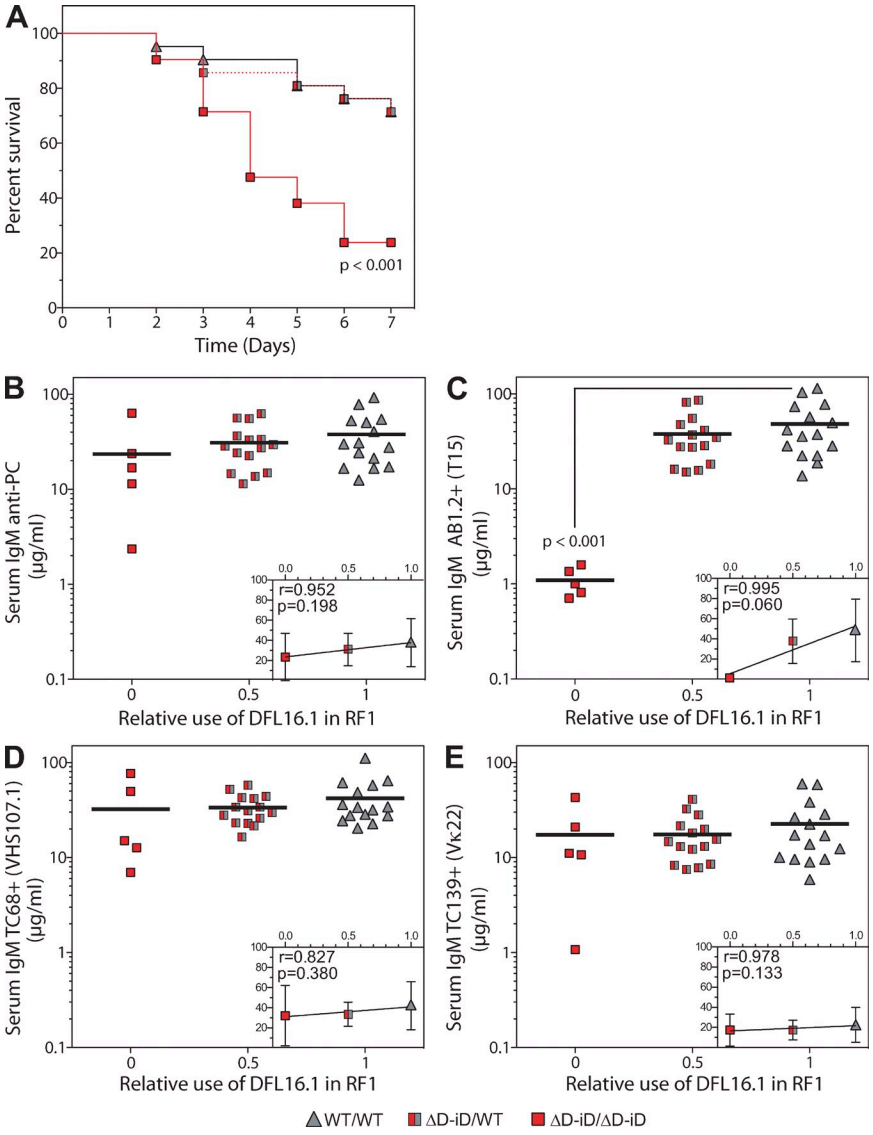

Figure 7. The availability of the *DFL16.1* sequence is critical for survival after challenge with live *S. pneumoniae*. (A) WT, homozygous, and heterozygous *ΔD-iD* mice were inoculated i.v. with live *S. pneumoniae* (strain A66.1), and survival was monitored. Serum was collected from the survivors 7 d after infection to measure the antibody levels. (B–E) Levels of serum IgM anti-PC (B), IgM expressing the T15-Id$^+$ (C), IgM antibodies dependent on the use of the heavy chain $V_HS107.1$ gene segments, TC68$^+$ (D), and IgM antibodies dependent on the use of the light chain $V_κ22$ gene segments, TC139$^+$ (E), in WT, heterozygous, and homozygous *ΔD-iD* mice that survived after challenge with live *S. pneumoniae* (strain A66.1). The levels of IgM antibodies for each mouse strain are plotted as a function of the relative use of *DFL16.1* in RF1 (*R* value). The horizontal lines indicate the mean value of each group. (inset plots) Mean serum concentrations (±SD) of IgM anti-PC, T15-Id$^+$, TC68$^+$, or TC139$^+$ from each mouse strain are presented as a function of *R* value. Levels of IgM antibodies are shown as an equivalent titer (μg/ml) to the BALB/c IgM anti-PC–producing hybridoma BH8 (Kearney et al., 1981). The data were combined from three independent experiments.

an exemplar of the role of NAbs in protection against both endogenous and exogenous deleterious antigens was instrumental to test our competing hypothesis. In the absence of evolutionary conserved D_H sequence, we find that somatic selection continues to elicit a set of NAbs capable of preventing the uptake of OxLDL by macrophages (Fig. 1). To the extent that this activity reflects the ability of these NAbs to function in normal cellular homeostasis, these data support the view that production of these NAbs is driven by self-antigen and somatic selection. Furthermore, the data suggest that access to conserved germline D_H sequence is not required to generate a fully functional physiological repertoire against self-antigens of this type.

In the case of the exogenous antigen, however, the answer proved quite different. Normal mice challenged with *S. pneumonia* produce high levels of protective anti-PC T15-Id$^+$ antibodies, mainly derived from B-1a cells (Briles et al., 1981; Kearney et al., 1981). The PC epitopes recognized by T15-Id$^+$ antibodies are found both on OxLDL as well on the bacteria cell wall. Accordingly, it has been suggested that the T15 clonotype has been conserved during evolution because of its value both for protection against host damage by oxidatively modified self-structures and for defense against infection with PC-bearing pathogens (Silverman et al., 2000). However, the severing of the relationship between the production of NAbs against OxLDL and NAbs against PC in our D_H-altered mice indicates that the concordance between these activities requires access to conserved germline D_H sequence content.

A recent study showed that deletion of the conserved $V_HS107.1$ gene, which is dominant among anti-PC antibodies, led to changes in epitope recognition on apoptotic cells (Chen et al., 2009). In light of our data, we suggest that the NAb repertoire produced in the absence of *DFL16.1* sequence no longer recognizes PC as the major phospholipid-related epitope on OxLDL, being hierarchically replaced, possibly by

an alternative epitope such as malondialdehyde (Chen et al., 2009). We propose that a large assortment of redundant anti-self NAbs reactive with alternative epitopes are available and able to play a role in tissue homeostasis, irrespective of the presence of evolutionary conserved gene segments. This suggests that major NAb clones, T15 in particular, have been fixed and predominant across evolution through natural selection for both homeostasis and host defense against common pathogens.

The serum concentration and quality of anti-PC antibodies in naive mice proved dependent on the availability of *DFL16.1* sequence. The analysis of the actual composition of the PC-specific heavy chain repertoire in B-1a cells from the D_H-altered mice revealed that, when there is forced reduction of availability to *DFL16.1* RF1 sequence, a compensatory increase in the frequencies of alternative V_H and J_H genes occurs that otherwise would be biased toward $V_HS107.1/J_H1$ gene usage (Crews et al., 1981). In mice forced to preferentially use charged CDR-H3s (*ΔD-iD*), we observed extensive exonucleolytic nibbling among the B-1a anti-PC transcripts to the extent that 30% of the anti-PC CDR-H3 sequences did not contain an identifiable *iD* sequence. We also observed a higher frequency of N-region additions compared with the non–anti-PC transcripts from B-1a cells (unpublished data). These findings reveal the existence of robust somatic selection operative on D_H-altered B cells and support the concept that the unusual CDR-H3 imposed by the *iD* transgene might inhibit the physiological humoral immune response to PC. Strikingly, we observed an increase in clonal diversity within the anti-PC B-1a cells as the *DFL16.1* gene segment became less available for use. Our findings therefore show that limiting the availability of an evolutionary conserved D_H element encoding a major B cell clonotype generates a whole new set of diversified B cell clones to fill the gap left by the missing clone. Thus, contrasting with the original nomenclature, the limitation/alteration of the D_H gene, defined as "D" for "diversity" (Cohn, 2008), which a priori would reduce the diversity of B cell precursors, led surprisingly to a more polyclonal and diversified response than the otherwise oligoclonal anti-PC immune response observed in WT animals (Cosenza and Köhler, 1972; Sher and Cohn, 1972; Gearhart et al., 1975; Crews et al., 1981).

Several mechanisms have been proposed to explain the T15 immunodominance in BALB/c mice, which is established early in ontogeny (Claflin and Berry, 1988; Feeney, 1991, 1992). This includes microhomology between the ends of the V_H and J_H gene segments and the ends of the D_H gene segments that, in the absence of N addition, drives rearrangement site preferences (Feeney, 1991). As a result, the prototypic T15 V-D and D-J junctions are the most common junctional sequences among $V_HS107.1$-$D_HDFL16.1$-J_H1 genes in neonatal B cells (Feeney, 1991). Likely because of both the high affinity of the T15 antibodies (Feeney and Thuerauf, 1989) and to the self-replenishing nature of the B-1a cells that produce them (Hayakawa et al., 1986b; Wemhoff and Quintans, 1987; Masmoudi et al., 1990; Kantor et al., 1995), it has been suggested that these characteristics would be sufficient to establish the T15 dominance for life (Kenny et al., 1992). As previously suggested, these limitations in the neonatal repertoire may have evolved to reproducibly provide certain specificities that are essentials for the survival of the species, supporting the idea of a layered immune system (Herzenberg and Herzenberg, 1989).

However, our findings reported here reopen this discussion and raise alternative interpretations. The *ΔD-DμFS* allele contains a single *DFL16.1* gene segment that has been doubly frameshifted to enable microhomology-driven rearrangement to preferentially access valine-enriched RF2 sequence in place of tyrosine-enriched RF1. Although access to the RF1 core is still possible, albeit at one-third the frequency, a termination codon was introduced into the third codon from the 3′ end of this RF, thereby destroying a part of the sequence used for the canonical T15 CDR-H. Thus, the rearrangement limitations of the neonatal B cell repertoire that normally ensure the conservation of the T15 clonotype have been subverted in *ΔD-DμFS* mice and require significant somatic modification to be allowed to contribute to the formation of classical T15 CDR-H3 amino acid sequence. Our finding of the T15 heavy chain prototype sequence among the *ΔD-DμFS* transcripts thus means that at least three of the mechanisms that normally limit the neonatal repertoire were subverted: (1) the aforementioned role of microhomology between V-D and D-J junctions, which would otherwise generate the hydrophobic-enriched RF2; (2) extensive exonucleolytic nibbling to eliminate the termination codon; and (3) addition of N nucleotides in the germline-enriched B-1a compartment to recreate the full DFL16.1 RF1 amino acid sequence. Indeed, we found additions of a "C" nucleotide at the V-D junction and "TC" nucleotides at the D-J junction, which completely abrogate the microhomology sites at both ends of the D_H, concomitantly recreating the T15 amino acid sequence. These observations suggest that there may be a sufficient imperative to create certain clonotypes within the NAb repertoire such that somatic selection can overcome germline limitations to recapitulate the lost "normal" repertoire. More importantly, these mechanisms of endogenous antigen-driven selection proved to be at work during immune homeostasis and powerful enough to be effective without any intentional immunization in the *ΔD-DμFS* mouse. However, this somatic drive clearly has limits because the *ΔD-iD* mouse, which completely lacks *DFL16.1* RF1 sequence, was unable to recreate this sequence, at least at the limits of our ability to detect it by flow cytometry and sequencing.

Unlike in the $V_HS107.1$ deficiency model (Mi et al., 2000), all immunized D_H-altered mice mounted a similar anti-PC response compared with the WT. More importantly, the anti-PC levels were indistinguishable between homozygous *ΔD-iD* and *ΔD-DFL* mice after immunization, even though the T15 response was not recovered in mice lacking the *DFL16.1* RF1 sequence altogether. Thus, the availability of *DFL16.1* core sequence proved to be necessary only to create a robust T15 response. The serum level of $TC139^+$ antibodies, reflecting the use of the $V_κ22$ light chain, was slightly increased in

ΔD-iD mice compared with the other mouse strains, suggesting a compensatory expansion of clones using the prototypic T15 light chain combined with heavy chains other than the canonical T15 $V_HS107.1$. The *ΔD-DμFS* mice, which can encode the V_H-T15 at the amino acid level, had serum levels of both anti-PC and T15-Id$^+$ antibodies comparable with WT after immunization. However, the variance in the T15-Id$^+$ antibody levels observed among the different *ΔD-DμFS* samples provides evidence for the difficulty in recapitulating the T15 clonotype in this mouse strain, possibly reflecting the low frequency of anti-PC T15-Id$^+$ B-1a cells, as illustrated in Fig. 3 (E and F) and at the sequence level in Fig. 4 C.

Our earlier experiments pointed out the importance of the NAb CDR-H3 in its germline configuration to provide immune protection against *S. pneumoniae* (Benedict and Kearney, 1999). Here we also tested the effects of the absence of *DFL16.1* gene segment on survival after challenge with live *S. pneumoniae*. The infected mice were able to produce abundant anti-PC antibodies, and both $V_HS107.1$ and $V_\kappa 22$ sequences were used. Although, our analysis limits conclusions about the antibody response of the initial cohort of mice, we found that 7 d after challenge with live bacteria, only the homozygous *ΔD-iD* mice were unable to produce T15-Id$^+$ antibodies. However, the anti-PC antibodies produced by these mice were less protective with significantly higher mortality observed in homozygous *ΔD-iD* compared with both heterozygous *ΔD-iD* and WT mice. Thus, naturally selected DFL16.1 germline sequence content is essential for the production of T15-Id$^+$ antibodies and is vital for mounting a successful defense against *S. pneumonia*.

Our findings provide the first evidence, to our knowledge, that the composition of the germline D_H locus, in concert with endogenous antigen-driven selection, can both qualitatively and quantitatively regulate the antigen-binding site features of the NAb repertoire and, by so doing, can control the ability of the host to protect against bacterial infection. However, the structural and chemical composition of the NAb paratope repertoire clearly differs, as demonstrated by our sequence analysis. One consequence of this divergence is the severing of the relationship between self-antigen recognition and protection against common pathogens, as illustrated by the T15 anti-PC response.

Collectively, these data may have important implications for the rational design of vaccines against hard-to-defend pathogens such as HIV. The first scenario, in which the protective B cell clones are not available, may help explain why classical vaccine intervention may not be able to easily create a protective immune response without requiring extensive somatic hypermutation (Mouquet et al., 2010; Scheid et al., 2011). Instead, classical vaccine protocols may be more likely to induce a polyclonal expansion of vaccine-specific B cells able to produce a diverse, albeit nonprotective and perhaps deleterious, antibody response (Nicoletti et al., 1993; Limpanasithikul et al., 1995; Putterman et al., 1996). In a second scenario in which the potentially protective B cell clones are available but at low frequencies or in nonchallenged B cell compartments, it is possible that vaccine protocols could be modified to elicit the desired responses at the levels needed to provide protection against future infections. In general, immunogen design will need to address the germline sequence–dependent likelihood of encountering or promoting high-affinity antibodies bearing antigen-binding sites that properly engage critical epitopes on the microorganism. Our D_H-altered mouse model provides one approach to testing these hypotheses and thus working out how essential aspects of B cell development and selection of the natural available repertoire influence vaccine responses and thus contribute to the likely success of rational vaccine strategies.

MATERIALS AND METHODS

Mice. The panel of D_H-altered *ΔD-DFL* (Schelonka et al., 2005), *ΔD-DμFS* (Schelonka et al., 2008; Zemlin et al., 2008), or *ΔD-iD* (Ippolito et al., 2006) backcrossed to BALB/c for 22 generations and WT BALB/c littermates were bred in our mouse colony at the University of Alabama at Birmingham (UAB). Animal care was conducted in accordance with established guidelines and protocols approved by the UAB Animal Care and Use Committee. Each mouse strain carries its unique D_H-altered allele as follows. The *ΔD-DFL* allele provides access to only the germline *DFL16.1* gene segment, increasing its contribution from 20% of the developing repertoire to 100%. The *ΔD-DμFS* allele contains a single *DFL16.1* gene segment that has been doubly frame-shifted to promote the use of valine-enriched RF2. Access to the RF1 sequence remains but at one-third the frequency and with the frameshift insertion of a termination codon at the third position from the 3′ terminus. In the *ΔD-iD* allele, the sequence of inverted *DSP2.2* has been embedded within *DFL16.1*. The *ΔD-iD* allele lacks the *DFL16.1* sequence altogether. Together, this panel of D_H-altered mice presents varying levels of availability of germline DFL16.1 sequence (0–100%).

The *R* value: relative use of *DFL16.1* in RF1. In WT BALB/c mice, the major T15 prototype uses germline *DFL16.1* RF1 sequence without N-region addition (Feeney, 1991). To perform quantitative calculations relating the likelihood of the use of *DFL16.1* RF1 sequence to the prevalence of antibodies bearing the T15-Id, we developed a parameter we term *R* value (Table 1), which reports the expected frequency of mature B cells using the *DFL16.1* in RF1 in our D_H-altered mice relative to WT. The calculation of *R* value takes into account the observed proportion of mature, recirculating IgM$^+$ IgD$^+$ B cells in the bone marrow relative to WT (R1), the expected frequency of use of the *DFL16.1* gene segment relative to WT (R2), and the frequency of use of *DFL16.1* in RF1 (R3), whether the mouse strain in question is homozygous or heterozygous for the mutant D_H allele. The *R* values for each genotype are represented in the Table 1 and were calculated based on previous published data (for *ΔD-DμFS* mice see Schelonka et al. [2008] and Zemlin et al. [2008], and for *ΔD-iD* mice see Ippolito et al. [2006]), according to the following formula:

$$R\text{ value} = \frac{R_{\text{alle A}}\left(\text{R1}\times\text{R2}\times\text{R3}\right) + R_{\text{alle B}}\left(\text{R1}\times\text{R2}\times\text{R3}\right)}{2}.$$

Serum assays of antibodies. The en bloc analysis of serum IgM reactivities was performed using a semiquantitative immunoblot assay. The method has been previously described (Nobrega et al., 1993; Haury et al., 1994, 1997). Specific antibody titers to OxLDL were determined by ELISA as previously described (Närvänen et al., 2001; Smook et al., 2008), using native LDL (Nat-LDL) and OxLDL (MyBioSource). Quantitative ELISA assays to determine the serum levels of anti-PC and T15-Id$^+$ antibodies were performed as previously described (Kearney et al., 1981; Desaymard et al., 1984). The following reagents were used: PC-BSA (high loaded PC-BSA), the monoclonal AB1.2 anti-idiotypic antibody against T15 (Kearney et al., 1981), the monoclonal antibody TC68 against $V_HS107.1$, and the monoclonal antibody TC139 against $V_\kappa 22$ (Desaymard et al., 1984). The levels of IgM

antibodies in each mouse strain are shown as an equivalent titer to the BALB/c IgM anti-PC–producing hybridoma BH8 (Kearney et al., 1981). The standard curve was used to calculate the equivalent titer of antibodies in each sample.

Macrophage binding/uptake assays. Binding/uptake of OxLDL to macrophages was assessed by three different approaches, immunoenzymatic, flow cytometry analysis, and confocal microscopy, based on several previous studies (Hörkkö et al., 1999; Binder et al., 2003; Miller et al., 2003; Xu et al., 2010). A murine macrophage cell line, RAW 264.7 (American Type Culture Collection), was used for all assays described, and the cells were cultured according to Xu et al. (2010). Immunoenzymatic assay was performed to assess the inhibition of binding of biotinylated-OxLDL (Biot-OxLDL) to 10^5 RAW macrophages plated in microtiter wells. To detect the 2 μg/ml Biot-OxLDL bound to RAW macrophages, we used streptavidin coupled with alkaline phosphatase, and the binding is expressed as OxLDL bound to macrophages in optical density at 405 nm. A flow cytometric approach was used to determine the inhibition of binding of 5 μg/ml Biot-OxLDL to 5×10^5 RAW macrophages. The intensity of fluorescence (streptavidin-PE) was indicative of Biot-OxLDL binding to macrophages. The inhibition of binding is depicted in the histogram graphs expressing the intensity of fluorescence, and the statistical analyses were performed using the mean fluorescence intensity of each sample, according to Xu et al. (2010). Confocal microscopy was used to determine the inhibition of binding/uptake of DiI-OxLDL by RAW macrophages. For nucleus staining, the cells were incubated for 10 min with 10 μg/ml DAPI (Sigma-Aldrich) and washed. The cells were then placed for confocal microscopy (LSM710; Carl Zeiss). For all three approaches, the binding/uptake of OxLDL to RAW macrophages was determined in the absence or presence of diluted pooled sera from each mouse strain. The specificity of the binding/uptake of OxLDL (either Biot- or DiI-OxLDL) was determined in the absence and presence of 50-fold unconjugated OxLDL or Nat-LDL as competitors.

Competition immunoassay. The specificity of IgM antibodies binding to PC and/or OxLDL was determined by competition immunoassays as described previously (Binder et al., 2003; Chou et al., 2009). In brief, sera from each mouse strain was pooled, diluted to 1:100, and incubated overnight at 4°C in the presence or absence of increasing concentrations of competitors. Samples were then centrifuged at 15,800 *g* for 45 min at 4°C, and supernatants were analyzed for binding to the respective antigen by ELISA.

Flow cytometry and cell sorting. Single-cell suspensions prepared from PerC and spleen were stained with the following fluorochrome-conjugated antibodies purchased from BD or eBioscience: anti-B220 PB (RA 3.6B2), anti-CD5 PE (53-7.3), anti–Mac-1 FITC (M1/70), and anti-CD138 PE (281-2). For anti-PC analysis, we used PC-DEX FITC (provided by J. Kenny, National Institute on Aging, National Institutes of Health, Baltimore, MD) and anti–T15-Id AB1.2 APC (Kearney et al., 1981). Analysis and sorting were then performed on an LSR II (BD) and MoFlo instrument (Dako), respectively. For B cell cultures, the cells were collected directly in sterile tubes containing RPMI medium and for mRNA purification the cells were collected directly in RLT lysis buffer (RNeasy mini-kit; QIAGEN).

B cell culture and LDA. Cultures of sorted B cell, stimulated with LPS, were performed as described previously (Vale et al., 2012). Sorted B cells were cultured at variable numbers in 24 replicates for each cell concentration, as follows: 18, 6, 2, and 0.66 B cells per well, to determine the frequency of IgM-secreting clones by ELISA according to Poisson's distribution and 10,000, 3,333, 1,111, 370, 123, 41, and 14 B cells per well to estimate the clonal frequencies of antigen-specific (PC) and/or idiotype-positive B cells (T15-Id$^+$) using ELISA. Culture supernatants were harvested usually on the ninth day of culture and analyzed by ELISA.

RT-PCR, cloning and sequencing. For each mouse strain, B-1a cells PC-DEX$^+$/AB1.2$^+$ diagonal high and low (see Fig. 4 A) were sorted directly into RLT lysis buffer. Cells were sorted from at least five mice per group and then pooled to achieve sufficient numbers of cells to allow for RNA extraction and sequencing. RNA isolation, RT-PCR amplification, and sequencing analysis were performed as previously described (Ivanov et al., 2005), except for the V_H primer. To screen for anti-PC Cμ transcripts without missing the true dimension of the repertoire, we intentionally used a V_H primer that biases toward the *V_HS107* family but also allows the amplification of other V_H family members (Feeney, 1990). In the present work, we used S107-1 primer 5′-GGTGAAGCTTGTGGAATCTGGAGGA-3′, as previously described by Feeney (1990). We used One-step RT-PCR kits (QIAGEN) for amplification. RT-PCR conditions were 50°C for 30 min, 95°C for 15 min, and then 95°C for 1 min, 55°C for 1 min, and 72°C for 1 min for 35 cycles, and then 72°C for 10 min. PCR products were cloned into TOPO-TA vector and transformed into TOP10 competent bacteria (Invitrogen). QIAprep Miniprep kits (QIAGEN) were used to isolate plasmid DNA from colonies. Plasmid DNAs were sequenced at the DNA Sequencing and Analysis Core at the UAB.

Immunization with heat-inactivated *S. pneumoniae*. A heat-inactivated preparation of strain R36A of *S. pneumoniae* was used. 8–12 wk-old WT, as well as *ΔD-DFL/ΔD-DFL*, *ΔD-DFL*/WT, *ΔD-DμFS/ΔD-DμFS*, *ΔD-DμFS*/WT, *ΔD-iD/ΔD-iD*, and *ΔD-iD*/WT mice, were immunized i.v. with 10^8 heat-inactivated/100 μl, pepsin-treated *S. pneumoniae* (strain R36A) as previously described (Briles et al., 1982). The number of mice in each group is given with the results. Blood was collected retroorbitally before and 7 d after infection. Mice were euthanized 7 d after immunization.

Infection with live *S. pneumoniae*. Live *S. pneumoniae* strain A66.1 was prepared according to Briles et al. (1981). 8–12 wk-old WT, homozygous *ΔD-iD*, and heterozygous *ΔD-iD*/WT mice were inoculated in the tail vein with 9,120–9,750 CFU/200 μl *S. pneumoniae* (strain A66.1). Blood was collected retroorbitally before and 7 d after infection. Mice were closely monitored for mortality until all surviving mice showed no signs of morbidity (hunched back, poor grooming, irritability, or unresponsiveness to touch), which occurred at 7 d after infection. Surviving mice were monitored daily for 21 d, at which time they were euthanized by CO_2 narcosis, followed by cervical dislocation.

Statistical analysis. Data were analyzed using SigmaPlot version 11 (SYSTAT Software, Inc). One-way ANOVA was performed if data in multiple groups were normally distributed with equal variance. The Kruskal-Wallis one-way ANOVA on ranks was used if three or more groups were compared and the data were not normally distributed with equal variance. If these tests indicated that the groups were significantly different, we used an All Pairwise Multiple Comparison Procedure, Holm-Sidak, or Dunn method, respectively, to determine which of the groups were significantly different from the others. Pearson's correlation coefficient r was calculated to evaluate relations. The Gehan-Breslow test was used to analyze survival after infection with live bacteria. Rejecting the null hypothesis at $\alpha = 0.05$ with a p-value < 0.05 was interpreted to indicate a significant difference.

Online supplemental material. Fig. S1 shows the immunoblot patterns of reactivity against self-antigens (brain extract) using IgM from sera and supernatants of B cell cultures from WT, *ΔD-DFL*, and *ΔD-iD* mice. Table S1, included as a separate Excel file, provides the CDR-H3 nucleotide sequences from VDJCμ transcripts cloned from PC-DEX^{lo}/AB1.2^{lo} and PC-DEX^{hi}/AB1.2^{hi} B-1a cells from each of the mouse strains; each of these CDR-H3 sequences is compared with the T15 prototype. Online supplemental material is available at http://www.jem.org/cgi/content/full/jem.20121861/DC1.

We thank members of the H.W. Schroeder Jr. laboratory for thoughtful discussion. We thank Dr. B. Dizon for invaluable advice and support. We are grateful to Y. Zhuang for expert technical assistance. We also thank J. King and members of the D.E. Briles laboratory for assistance challenging with live bacteria. We thank S.L. Dong for advice with the experiments involving macrophage uptake and

microscopy. We are grateful for the aid of the Comprehensive Flow Cytometry Core (AR43311) and the DNA Sequencing and Analysis Core (CA13148) at the University of Alabama at Birmingham.

This work was supported in part by National Institutes of Health grants NIH-AI048115 (to H.W. Schroeder Jr.), AI088498 (to H.W. Schroeder Jr.), AI090742 (to H.W. Schroeder Jr.), AI021458 (to D.E. Briles), AI14782 (to J.F. Kearney), and AI100076-01 (to P.D. Burrows). M. Zemlin was supported in part by the German Research Council, Transregio 22, project A17. A. Nobrega was partially supported by Conselho Nacional de Desenvolvimento Científico e Tecnológico (CNPq)/Brazil, Fundação de Amparo à Pesquisa do Estado do Rio de Janeiro, and Financiadora de Estudos e Projetos. A.M. Vale was supported in part by a fellowship from Coordenação de Aperfeiçoamento de Pessoal de Nível Superior/Brazil and by an exchange-training fellowship from CNPq.

The authors have no conflicting financial interests.

Submitted: 16 August 2012
Accepted: 6 March 2013

REFERENCES

Aprahamian, T., I. Rifkin, R. Bonegio, B. Hugel, J.M. Freyssinet, K. Sato, J.J. Castellot Jr., and K. Walsh. 2004. Impaired clearance of apoptotic cells promotes synergy between atherogenesis and autoimmune disease. *J. Exp. Med.* 199:1121–1131. http://dx.doi.org/10.1084/jem.20031557

Avrameas, S. 1991. Natural autoantibodies: from 'horror autotoxicus' to 'gnothi seauton'. *Immunol. Today.* 12:154–159.

Bachmann, M.F., U. Kalinke, A. Althage, G. Freer, C. Burkhart, H. Roost, M. Aguet, H. Hengartner, and R.M. Zinkernagel. 1997. The role of antibody concentration and avidity in antiviral protection. *Science.* 276:2024–2027. http://dx.doi.org/10.1126/science.276.5321.2024

Baumgarth, N. 2011. The double life of a B-1 cell: self-reactivity selects for protective effector functions. *Nat. Rev. Immunol.* 11:34–46. http://dx.doi.org/10.1038/nri2901

Benedict, C.L., and J.F. Kearney. 1999. Increased junctional diversity in fetal B cells results in a loss of protective anti-phosphorylcholine antibodies in adult mice. *Immunity.* 10:607–617. http://dx.doi.org/10.1016/S1074-7613(00)80060-6

Binder, C.J., and G.J. Silverman. 2005. Natural antibodies and the autoimmunity of atherosclerosis. *Springer Semin. Immunopathol.* 26:385–404. http://dx.doi.org/10.1007/s00281-004-0185-z

Binder, C.J., S. Hörkkö, A. Dewan, M.K. Chang, E.P. Kieu, C.S. Goodyear, P.X. Shaw, W. Palinski, J.L. Witztum, and G.J. Silverman. 2003. Pneumococcal vaccination decreases atherosclerotic lesion formation: molecular mimicry between *Streptococcus pneumoniae* and oxidized LDL. *Nat. Med.* 9:736–743. http://dx.doi.org/10.1038/nm876

Bos, N.A., H. Kimura, C.G. Meeuwsen, H. De Visser, M.P. Hazenberg, B.S. Wostmann, J.R. Pleasants, R. Benner, and D.M. Marcus. 1989. Serum immunoglobulin levels and naturally occurring antibodies against carbohydrate antigens in germ-free BALB/c mice fed chemically defined ultrafiltered diet. *Eur. J. Immunol.* 19:2335–2339. http://dx.doi.org/10.1002/eji.1830191223

Briles, D.E., M. Nahm, K. Schroer, J. Davie, P. Baker, J. Kearney, and R. Barletta. 1981. Antiphosphocholine antibodies found in normal mouse serum are protective against intravenous infection with type 3 *Streptococcus pneumoniae*. *J. Exp. Med.* 153:694–705. http://dx.doi.org/10.1084/jem.153.3.694

Briles, D.E., C. Forman, S. Hudak, and J.L. Claflin. 1982. Anti-phosphorylcholine antibodies of the T15 idiotype are optimally protective against *Streptococcus pneumoniae*. *J. Exp. Med.* 156:1177–1185. http://dx.doi.org/10.1084/jem.156.4.1177

Chen, Y., Y.B. Park, E. Patel, and G.J. Silverman. 2009. IgM antibodies to apoptosis-associated determinants recruit C1q and enhance dendritic cell phagocytosis of apoptotic cells. *J. Immunol.* 182:6031–6043. http://dx.doi.org/10.4049/jimmunol.0804191

Choi, Y.S., J.A. Dieter, K. Rothaeusler, Z. Luo, and N. Baumgarth. 2012. B-1 cells in the bone marrow are a significant source of natural IgM. *Eur. J. Immunol.* 42:120–129. http://dx.doi.org/10.1002/eji.201141890

Chou, M.Y., L. Fogelstrand, K. Hartvigsen, L.F. Hansen, D. Woelkers, P.X. Shaw, J. Choi, T. Perkmann, F. Bäckhed, Y.I. Miller, et al. 2009. Oxidation-specific epitopes are dominant targets of innate natural antibodies in mice and humans. *J. Clin. Invest.* 119:1335–1349. http://dx.doi.org/10.1172/JCI36800

Claflin, J.L., and J. Berry. 1988. Genetics of the phosphocholine-specific antibody response to *Streptococcus pneumoniae*. Germ-line but not mutated T15 antibodies are dominantly selected. *J. Immunol.* 141:4012–4019.

Cohn, M. 2008. A hypothesis accounting for the paradoxical expression of the D gene segment in the BCR and the TCR. *Eur. J. Immunol.* 38:1779–1787. http://dx.doi.org/10.1002/eji.200738089

Cosenza, H., and H. Köhler. 1972. Specific inhibition of plaque formation to phosphorylcholine by antibody against antibody. *Science.* 176:1027–1029. http://dx.doi.org/10.1126/science.176.4038.1027

Crews, S., J. Griffin, H. Huang, K. Calame, and L. Hood. 1981. A single VH gene segment encodes the immune response to phosphorylcholine: somatic mutation is correlated with the class of the antibody. *Cell.* 25:59–66. http://dx.doi.org/10.1016/0092-8674(81)90231-2

de Faire, U., J. Su, X. Hua, A. Frostegård, M. Halldin, M.L. Hellenius, M. Wikström, I. Dahlbom, H. Grönlund, and J. Frostegård. 2010. Low levels of IgM antibodies to phosphorylcholine predict cardiovascular disease in 60-year old men: effects on uptake of oxidized LDL in macrophages as a potential mechanism. *J. Autoimmun.* 34:73–79. http://dx.doi.org/10.1016/j.jaut.2009.05.003

Desaymard, C., A.M. Giusti, and M.D. Scharff. 1984. Rat anti-T15 monoclonal antibodies with specificity for V_H- and V_H-V_L epitopes. *Mol. Immunol.* 21:961–967. http://dx.doi.org/10.1016/0161-5890(84)90154-8

Feeney, A.J. 1990. Lack of N regions in fetal and neonatal mouse immunoglobulin V-D-J junctional sequences. *J. Exp. Med.* 172:1377–1390. http://dx.doi.org/10.1084/jem.172.5.1377

Feeney, A.J. 1991. Predominance of the prototypic T15 anti-phosphorylcholine junctional sequence in neonatal pre-B cells. *J. Immunol.* 147:4343–4350.

Feeney, A.J. 1992. Predominance of VH-D-JH junctions occurring at sites of short sequence homology results in limited junctional diversity in neonatal antibodies. *J. Immunol.* 149:222–229.

Feeney, A.J., and D.J. Thuerauf. 1989. Sequence and fine specificity analysis of primary 511 anti-phosphorylcholine antibodies. *J. Immunol.* 143:4061–4068.

Feeney, A.J., S.H. Clarke, and D.E. Mosier. 1988. Specific H chain junctional diversity may be required for non-T15 antibodies to bind phosphorylcholine. *J. Immunol.* 141:1267–1272.

Gearhart, P.J., N.H. Sigal, and N.R. Klinman. 1975. Heterogeneity of the BALB/c antiphosphorylcholine antibody response at the precursor cell level. *J. Exp. Med.* 141:56–71. http://dx.doi.org/10.1084/jem.141.1.56

Haas, K.M., J.C. Poe, D.A. Steeber, and T.F. Tedder. 2005. B-1a and B-1b cells exhibit distinct developmental requirements and have unique functional roles in innate and adaptive immunity to *S. pneumoniae*. *Immunity.* 23:7–18. http://dx.doi.org/10.1016/j.immuni.2005.04.011

Haury, M., A. Grandien, A. Sundblad, A. Coutinho, and A. Nobrega. 1994. Global analysis of antibody repertoires. 1. An immunoblot method for the quantitative screening of a large number of reactivities. *Scand. J. Immunol.* 39:79–87. http://dx.doi.org/10.1111/j.1365-3083.1994.tb03343.x

Haury, M., A. Sundblad, A. Grandien, C. Barreau, A. Coutinho, and A. Nobrega. 1997. The repertoire of serum IgM in normal mice is largely independent of external antigenic contact. *Eur. J. Immunol.* 27:1557–1563. http://dx.doi.org/10.1002/eji.1830270635

Hayakawa, K., R.R. Hardy, M. Honda, L.A. Herzenberg, A.D. Steinberg, and L.A. Herzenberg. 1984. Ly-1 B cells: functionally distinct lymphocytes that secrete IgM autoantibodies. *Proc. Natl. Acad. Sci. USA.* 81:2494–2498. http://dx.doi.org/10.1073/pnas.81.8.2494

Hayakawa, K., R.R. Hardy, and L.A. Herzenberg. 1986a. Peritoneal Ly-1 B cells: genetic control, autoantibody production, increased lambda light chain expression. *Eur. J. Immunol.* 16:450–456. http://dx.doi.org/10.1002/eji.1830160423

Hayakawa, K., R.R. Hardy, A.M. Stall, L.A. Herzenberg, and L.A. Herzenberg. 1986b. Immunoglobulin-bearing B cells reconstitute and maintain the murine Ly-1 B cell lineage. *Eur. J. Immunol.* 16:1313–1316. http://dx.doi.org/10.1002/eji.1830161021

Hayakawa, K., M. Asano, S.A. Shinton, M. Gui, D. Allman, C.L. Stewart, J. Silver, and R.R. Hardy. 1999. Positive selection of natural

autoreactive B cells. *Science*. 285:113–116. http://dx.doi.org/10.1126/science.285.5424.113

Herzenberg, L.A., and L.A. Herzenberg. 1989. Toward a layered immune system. *Cell*. 59:953–954. http://dx.doi.org/10.1016/0092-8674(89)90748-4

Hörkkö, S., D.A. Bird, E. Miller, H. Itabe, N. Leitinger, G. Subbanagounder, J.A. Berliner, P. Friedman, E.A. Dennis, L.K. Curtiss, et al. 1999. Monoclonal autoantibodies specific for oxidized phospholipids or oxidized phospholipid-protein adducts inhibit macrophage uptake of oxidized low-density lipoproteins. *J. Clin. Invest.* 103:117–128. http://dx.doi.org/10.1172/JCI4533

Ippolito, G.C., R.L. Schelonka, M. Zemlin, I.I. Ivanov, R. Kobayashi, C. Zemlin, G.L. Gartland, L. Nitschke, J. Pelkonen, K. Fujihashi, et al. 2006. Forced usage of positively charged amino acids in immunoglobulin CDR-H3 impairs B cell development and antibody production. *J. Exp. Med.* 203:1567–1578. http://dx.doi.org/10.1084/jem.20052217

Ivanov, I.I., R.L. Schelonka, Y. Zhuang, G.L. Gartland, M. Zemlin, and H.W. Schroeder Jr. 2005. Development of the expressed Ig CDR-H3 repertoire is marked by focusing of constraints in length, amino acid use, and charge that are first established in early B cell progenitors. *J. Immunol.* 174:7773–7780.

Kantor, A.B., A.M. Stall, S. Adams, K. Watanabe, and L.A. Herzenberg. 1995. De novo development and self-replenishment of B cells. *Int. Immunol.* 7:55–68. http://dx.doi.org/10.1093/intimm/7.1.55

Kantor, A.B., C.E. Merrill, L.A. Herzenberg, and J.L. Hillson. 1997. An unbiased analysis of V(H)-D-J(H) sequences from B-1a, B-1b, and conventional B cells. *J. Immunol.* 158:1175–1186.

Kaveri, S.V., G.J. Silverman, and J. Bayry. 2012. Natural IgM in immune equilibrium and harnessing their therapeutic potential. *J. Immunol.* 188:939–945. http://dx.doi.org/10.4049/jimmunol.1102107

Kearney, J.F. 2005. Innate-like B cells. *Springer Semin. Immunopathol.* 26:377–383. http://dx.doi.org/10.1007/s00281-004-0184-0

Kearney, J.F., R. Barletta, Z.S. Quan, and J. Quintáns. 1981. Monoclonal vs. heterogeneous anti-H-8 antibodies in the analysis of the anti-phosphorylcholine response in BALB/c mice. *Eur. J. Immunol.* 11:877–883. http://dx.doi.org/10.1002/eji.1830111106

Kenny, J.J., C.M. Moratz, G. Guelde, C.D. O'Connell, J. George, C. Dell, S.J. Penner, J.S. Weber, J. Berry, J.L. Claflin, et al. 1992. Antigen binding and idiotype analysis of antibodies obtained after electroporation of heavy and light chain genes encoding phosphocholine-specific antibodies: a model for T15-idiotype dominance. *J. Exp. Med.* 176:1637–1643. http://dx.doi.org/10.1084/jem.176.6.1637

Kyaw, T., C. Tay, S. Krishnamurthi, P. Kanellakis, A. Agrotis, P. Tipping, A. Bobik, and B.H. Toh. 2011. B1a B lymphocytes are atheroprotective by secreting natural IgM that increases IgM deposits and reduces necrotic cores in atherosclerotic lesions. *Circ. Res.* 109:830–840. http://dx.doi.org/10.1161/CIRCRESAHA.111.248542

Lévy, M. 1984. Frequencies of phosphorylcholine-specific and T15-associated 10/13 idiotope-positive B cells within lipopolysaccharide-reactive B cells of adult BALB/c mice. *Eur. J. Immunol.* 14:864–868. http://dx.doi.org/10.1002/eji.1830140917

Limpanasithikul, W., S. Ray, and B. Diamond. 1995. Cross-reactive antibodies have both protective and pathogenic potential. *J. Immunol.* 155: 967–973.

Masmoudi, H., T. Mota-Santos, F. Huetz, A. Coutinho, and P.A. Cazenave. 1990. All T15 Id-positive antibodies (but not the majority of VHT15+ antibodies) are produced by peritoneal CD5+ B lymphocytes. *Int. Immunol.* 2:515–520. http://dx.doi.org/10.1093/intimm/2.6.515

McDaniel, L.S., W.H. Benjamin Jr., C. Forman, and D.E. Briles. 1984. Blood clearance by anti-phosphocholine antibodies as a mechanism of protection in experimental pneumococcal bacteremia. *J. Immunol.* 133: 3308–3312.

Mi, Q.S., L. Zhou, D.H. Schulze, R.T. Fischer, A. Lustig, L.J. Rezanka, D.M. Donovan, D.L. Longo, and J.J. Kenny. 2000. Highly reduced protection against *Streptococcus pneumoniae* after deletion of a single heavy chain gene in mouse. *Proc. Natl. Acad. Sci. USA*. 97:6031–6036. http://dx.doi.org/10.1073/pnas.110039497

Miller, Y.I., S. Viriyakosol, C.J. Binder, J.R. Feramisco, T.N. Kirkland, and J.L. Witztum. 2003. Minimally modified LDL binds to CD14, induces macrophage spreading via TLR4/MD-2, and inhibits phagocytosis of apoptotic cells. *J. Biol. Chem.* 278:1561–1568. http://dx.doi.org/10.1074/jbc.M209634200

Mouquet, H., J.F. Scheid, M.J. Zoller, M. Krogsgaard, R.G. Ott, S. Shukair, M.N. Artyomov, J. Pietzsch, M. Connors, F. Pereyra, et al. 2010. Polyreactivity increases the apparent affinity of anti-HIV antibodies by heteroligation. *Nature*. 467:591–595. http://dx.doi.org/10.1038/nature09385

Mouthon, L., A. Nobrega, N. Nicolas, S.V. Kaveri, C. Barreau, A. Coutinho, and M.D. Kazatchkine. 1995. Invariance and restriction toward a limited set of self-antigens characterize neonatal IgM antibody repertoires and prevail in autoreactive repertoires of healthy adults. *Proc. Natl. Acad. Sci. USA*. 92:3839–3843. http://dx.doi.org/10.1073/pnas.92.9.3839

Närvänen, O., A. Erkkilä, and S. Ylä-Herttuala. 2001. Evaluation and characterization of EIA measuring autoantibodies against oxidized LDL. *Free Radic. Biol. Med.* 31:769–777. http://dx.doi.org/10.1016/S0891-5849(01)00636-0

Nicoletti, C., X. Yang, and J. Cerny. 1993. Repertoire diversity of antibody response to bacterial antigens in aged mice. III. Phosphorylcholine antibody from young and aged mice differ in structure and protective activity against infection with *Streptococcus pneumoniae*. *J. Immunol.* 150:543–549.

Nobrega, A., M. Haury, A. Grandien, E. Malanchère, A. Sundblad, and A. Coutinho. 1993. Global analysis of antibody repertoires. II. Evidence for specificity, self-selection and the immunological "homunculus" of antibodies in normal serum. *Eur. J. Immunol.* 23:2851–2859. http://dx.doi.org/10.1002/eji.1830231119

Ochsenbein, A.F., T. Fehr, C. Lutz, M. Suter, F. Brombacher, H. Hengartner, and R.M. Zinkernagel. 1999. Control of early viral and bacterial distribution and disease by natural antibodies. *Science*. 286:2156–2159. http://dx.doi.org/10.1126/science.286.5447.2156

Potter, M., and M.A. Leon. 1968. Three IgA myeloma immunoglobulins from the BALB/ mouse: precipitation with pneumococcal C polysaccharide. *Science*. 162:369–371. http://dx.doi.org/10.1126/science.162.3851.369

Putterman, C., W. Limpanasithikul, M. Edelman, and B. Diamond. 1996. The double edged sword of the immune response: mutational analysis of a murine anti-pneumococcal, anti-DNA antibody. *J. Clin. Invest.* 97:2251–2259. http://dx.doi.org/10.1172/JCI118666

Rapaka, R.R., D.M. Ricks, J.F. Alcorn, K. Chen, S.A. Khader, M. Zheng, S. Plevy, E. Bengtén, and J.K. Kolls. 2010. Conserved natural IgM antibodies mediate innate and adaptive immunity against the opportunistic fungus *Pneumocystis murina*. *J. Exp. Med.* 207:2907–2919. http://dx.doi.org/10.1084/jem.20100034

Scheid, J.F., H. Mouquet, B. Ueberheide, R. Diskin, F. Klein, T.Y. Oliveira, J. Pietzsch, D. Fenyo, A. Abadir, K. Velinzon, et al. 2011. Sequence and structural convergence of broad and potent HIV antibodies that mimic CD4 binding. *Science*. 333:1633–1637. http://dx.doi.org/10.1126/science.1207227

Schelonka, R.L., I.I. Ivanov, D.H. Jung, G.C. Ippolito, L. Nitschke, Y. Zhuang, G.L. Gartland, J. Pelkonen, F.W. Alt, K. Rajewsky, and H.W. Schroeder Jr. 2005. A single DH gene segment creates its own unique CDR-H3 repertoire and is sufficient for B cell development and immune function. *J. Immunol.* 175:6624–6632.

Schelonka, R.L., J. Tanner, Y. Zhuang, G.L. Gartland, M. Zemlin, and H.W. Schroeder Jr. 2007. Categorical selection of the antibody repertoire in splenic B cells. *Eur. J. Immunol.* 37:1010–1021. http://dx.doi.org/10.1002/eji.200636569

Schelonka, R.L., M. Zemlin, R. Kobayashi, G.C. Ippolito, Y. Zhuang, G.L. Gartland, A. Szalai, K. Fujihashi, K. Rajewsky, and H.W. Schroeder Jr. 2008. Preferential use of DH reading frame 2 alters B cell development and antigen-specific antibody production. *J. Immunol.* 181:8409–8415.

Schroeder, H.W. Jr., M. Zemlin, M. Khass, H.H. Nguyen, and R.L. Schelonka. 2010. Genetic control of DH reading frame and its effect on B-cell development and antigen-specific antibody production. *Crit. Rev. Immunol.* 30:327–344. http://dx.doi.org/10.1615/CritRevImmunol.v30.i4.20

Shaw, P.X., S. Hörkkö, M.K. Chang, L.K. Curtiss, W. Palinski, G.J. Silverman, and J.L. Witztum. 2000. Natural antibodies with the T15 idiotype may act in atherosclerosis, apoptotic clearance, and protective immunity. *J. Clin. Invest.* 105:1731–1740. http://dx.doi.org/10.1172/JCI8472

Sher, A., and M. Cohn. 1972. Inheritance of an idiotype associated with the immune response of inbred mice to phosphorylcholine. *Eur. J. Immunol.* 2:319–326. http://dx.doi.org/10.1002/eji.1830020405

Sidman, C.L., L.D. Shultz, R.R. Hardy, K. Hayakawa, and L.A. Herzenberg. 1986. Production of immunoglobulin isotypes by Ly-1+ B cells in viable motheaten and normal mice. *Science.* 232:1423–1425. http://dx.doi.org/10.1126/science.3487115

Sigal, N.H., P.J. Gearhart, and N.R. Klinman. 1975. The frequency of phosphorylcholine-specific B cells in conventional and germfree BALB/C mice. *J. Immunol.* 114:1354–1358.

Sigal, N.H., A.R. Pickard, E.S. Metcalf, P.J. Gearhart, and N.R. Klinman. 1977. Expression of phosphorylcholine-specific B cells during murine development. *J. Exp. Med.* 146:933–948. http://dx.doi.org/10.1084/jem.146.4.933

Silverman, G.J., S.P. Cary, D.C. Dwyer, L. Luo, R. Wagenknecht, and V.E. Curtiss. 2000. A B cell superantigen–induced persistent "Hole" in the B-1 repertoire. *J. Exp. Med.* 192:87–98. http://dx.doi.org/10.1084/jem.192.1.87

Smook, M.L., M. van Leeuwen, P. Heeringa, J.G. Damoiseaux, R. Theunissen, M.J. Daemen, E. Lutgens, and J.W. Tervaert. 2008. Anti-oxLDL antibody isotype levels, as potential markers for progressive atherosclerosis in APOE and APOECD40L mice. *Clin. Exp. Immunol.* 154:264–269. http://dx.doi.org/10.1111/j.1365-2249.2008.03746.x

Tornberg, U.C., and D. Holmberg. 1995. B-1a, B-1b and B-2 B cells display unique VHDJH repertoires formed at different stages of ontogeny and under different selection pressures. *EMBO J.* 14:1680–1689.

Vale, A.M., J.M. Tanner, R.L. Schelonka, Y. Zhuang, M. Zemlin, G.L. Gartland, and H.W. Schroeder Jr. 2010. The peritoneal cavity B-2 antibody repertoire appears to reflect many of the same selective pressures that shape the B-1a and B-1b repertoires. *J. Immunol.* 185:6085–6095. http://dx.doi.org/10.4049/jimmunol.1001423

Vale, A.M., J.B. Foote, A. Granato, Y. Zhuang, R.M. Pereira, U.G. Lopes, M. Bellio, P.D. Burrows, H.W. Schroeder Jr., and A. Nobrega. 2012. A rapid and quantitative method for the evaluation of V gene usage, specificities and the clonal size of B cell repertoires. *J. Immunol. Methods.* 376:143–149. http://dx.doi.org/10.1016/j.jim.2011.12.005

Wemhoff, G.A., and J. Quintans. 1987. Alterations of idiotypic profiles: the cellular basis of T15 dominance in BALB/c mice. *J. Mol. Cell. Immunol.* 3:307–320.

Xu, S., Y. Huang, Y. Xie, T. Lan, K. Le, J. Chen, S. Chen, S. Gao, X. Xu, X. Shen, et al. 2010. Evaluation of foam cell formation in cultured macrophages: an improved method with Oil Red O staining and DiI-oxLDL uptake. *Cytotechnology.* 62:473–481. http://dx.doi.org/10.1007/s10616-010-9290-0

Zemlin, M., R.L. Schelonka, G.C. Ippolito, C. Zemlin, Y. Zhuang, G.L. Gartland, L. Nitschke, J. Pelkonen, K. Rajewsky, and H.W. Schroeder Jr. 2008. Regulation of repertoire development through genetic control of DH reading frame preference. *J. Immunol.* 181:8416–8424.

Zhou, Z.H., Y. Zhang, Y.F. Hu, L.M. Wahl, J.O. Cisar, and A.L. Notkins. 2007. The broad antibacterial activity of the natural antibody repertoire is due to polyreactive antibodies. *Cell Host Microbe.* 1:51–61. http://dx.doi.org/10.1016/j.chom.2007.01.002